

# Methanogenesis by CO<sub>2</sub> reduction dominates lake sediments with different organic matter compositions

Guangyi Su<sup>1\*</sup>, Julie Tolu<sup>2</sup>, Clemens Glombitza<sup>3</sup>, Jakob Zopfi<sup>4</sup>, Moritz F. Lehmann<sup>4</sup>,  
Mark A. Lever<sup>3</sup>, Carsten J. Schubert<sup>1, 3</sup>

<sup>1</sup> Swiss Federal Institute of Aquatic Science and Technology (EAWAG), Department of Surface Waters – Research and Management, 6047 Kastanienbaum, Switzerland

<sup>2</sup> Swiss Federal Institute of Aquatic Science and Technology (EAWAG), Department of Water resources and Drinking water, 8600 Duebendorf, Switzerland

<sup>3</sup> Institute of Biogeochemistry and Pollutant Dynamics, ETH Zurich, 8092 Zurich, Switzerland

<sup>4</sup> Department of Environmental Sciences, University of Basel, 4056 Basel, Switzerland

\*corresponding author: Guangyi Su, [guangyi.su@unibas.ch](mailto:guangyi.su@unibas.ch)

## Abstract

Microbial methane production is a respiration reaction involved in the terminal step of anaerobic degradation of organic matter. Due to the dependency of methanogenic substrate production on fermentation reactions that produce different end productions, different sources and compositions of organic carbon (OC) may impact the methanogenic potential in lake sediments. Here, we investigate the sources and compositions of OC in sediments of Lake Geneva and how both are potentially linked to methane production. Differences in dominant long-chain fatty acid abundances and carbon isotopic compositions suggest the predominance of diagenetically altered phytoplankton-derived OC at a profundal site and temporally highly variable sources of both aquatic and terrestrial OC in a deltaic location. Despite these differences, radiotracer-based methanogenesis rate measurements and stable isotopic signatures of methane indicate significant methane production that is dominated by CO<sub>2</sub> reduction (>95% of total methanogenesis) in both locations. Matching this interpretation, members of well-known CO<sub>2</sub>-reducing *Methanoregula* sp. dominate both sites. No clear effect of OC source on methane production rates was evident. Our data demonstrate that OC of diverse sources and diagenetic states support microbial methane production, but do not indicate a clear impact of the OC source on the dominant methanogenic pathway or the community structure of methanogenic microorganisms in lacustrine sediments.

Keywords: Methane production rate; Methanogenesis pathway; Sediment organic carbon; Lipid biomarkers; Methanogen community

## 1. Introduction

Lakes represent an important source of methane (CH<sub>4</sub>) to the atmosphere (Bastviken et al., 2011), which is a potent greenhouse gas with a global warming potential more than 27 times that of carbon dioxide on a 100-year basis (GWP-100) (Masson-Delmotte et al., 2021). Although recent evidence suggests that various living organisms can produce methane under oxic conditions (Ernst et al., 2022), most CH<sub>4</sub> in lakes is still produced primarily during the anaerobic decomposition of organic carbon (OC) in sediments, from where it escapes by ebullition or diffusion into the bottom waters. Methane formation is the final step in the degradation of organic matter, and is catalyzed by anaerobic methanogenic archaea, capable of using several substrates including H<sub>2</sub>/CO<sub>2</sub>, acetate, and methylated compounds (Lyu et al., 2018). It is still poorly understood how methane production in lake sediments is regulated, and to what extent the methanogenic potential is related to OC quality. In this regard, microbial organic matter degradation reactions (e.g., hydrolysis, fermentation, and anaerobic oxidation) play a critical role by sequentially breaking down organic macromolecules, such as proteins, carbohydrates, and lipids, to acetate and H<sub>2</sub>/CO<sub>2</sub>, which are then used as substrates by methanogenic archaea (Demirel and Scherer, 2008).

Freshwater lakes cover only a small portion of the Earth's surface (< 3%) (Downing et al., 2006), compared to oceans (71%), yet, the annually accumulated OC in lakes represents nearly half of what is stored in the oceans (Mendonça et al., 2017). In many lakes, most of organic matter in sediments is derived from autochthonous aquatic organisms like phytoplankton and aquatic macrophytes (Dean and Gorham, 1998). On the other hand, allochthonous organic carbon such as detritus of terrestrial vegetation can account for a significant fraction of the lacustrine sedimentary organic matter (Larsen et al., 2011), for example within river deltas (Randlett et al., 2015). In small or oligotrophic lakes and/or high-latitude/altitude lakes, OC sedimentation may in fact be dominated by land-derived organic matter, and it has previously been observed that high carbon burial efficiency in sediments is linked to a high proportion of allochthonous OC (Sobek et al., 2009). In general, OC from aquatic biomass such as

phytoplankton mainly comprises relatively labile compounds (Parsons et al., 1961). In contrast, allochthonous OC (e.g., terrestrial plants) contains more complex structural and biochemically recalcitrant compounds, such as cellulose and lignin (Opsahl and Benner, 1995), which are more effectively preserved over time (Han et al., 2020, 2022). The different biochemical compositions and characteristics of OC in lake sediments, and the associated differential susceptibility to hydrolytic attack and microbial breakdown into smaller carbon compounds (Lehmann et al., 2002, 2020), might substantially affect CH<sub>4</sub> production and emission, as has been suggested in previous studies (Grasset et al., 2018; West et al., 2012). However, laboratory experiments performed at short-time scales (i.e., within weeks or months), involving the spiking of sediments with fresh algal and/or plant organic materials, do not accurately reflect effects of enhanced OC contribution to natural sediments on CH<sub>4</sub> production. This is because the compositions and lability of original organic materials may vary greatly after sedimentation due to oxidative destruction and microbial alteration during sinking in the water column (Kawamura et al., 1987). Moreover, allochthonous OC found in lake sediments is often the less-reactive (i.e. less bio-degradable) remnant of land-derived debris, where the more reactive fractions have already been removed on land or during fluvial transport (Raymond and Bauer, 2001). Lastly, while it is known that organic matter bioavailability decreases over time, as labile components are selectively remineralized (Grasset et al., 2018), the effects of organic matter quality and OC degradation state, and their interactions, on CH<sub>4</sub> production remain uncertain.

Lipid biomarkers and their stable carbon isotopic composition can be used to infer sources and diagenetic state of lacustrine organic matter (Dai et al., 2005; Meyers and Ishiwatari, 1993). Different chain lengths of fatty acids and n-alkanes can be used for the distinction between aquatic phytoplankton and terrestrial plants (Cranwell, 1976; Eglinton and Hamilton, 1967). In addition, primary producers growing in different habitats (e.g., terrestrial plants and freshwater phytoplankton) have distinct isotopic compositions, due to the differences in C sources and biochemical pathways, through which inorganic carbon is assimilated and incorporated into biomass (Cloern et al., 2002). For example, terrestrial C<sub>3</sub> plants incorporate carbon dioxide from the atmosphere using the C<sub>3</sub> Calvin-Benson pathway and consequently have an average bulk isotopic value of ca -28‰, while isotopic values of various aquatic plants are often significantly less negative (e.g., an average of -20‰ for benthic diatoms) (Cloern et al., 2002; O’Leary, 1981). Moreover, stable carbon isotope measurements can be used to

trace the carbon flow from organic matter degradation to CH<sub>4</sub> in lake sediments. The isotopic signatures of methane and methane precursors (e.g., dissolved inorganic carbon, bulk organic carbon) can be used to assess the relative contribution of the major pathways (i.e., CO<sub>2</sub> reduction and acetoclastic methanogenesis) to total CH<sub>4</sub> production (Conrad, 2005; Whiticar, 1999). To date it remains unclear, which organic compounds represent the main precursors of molecules that are ultimately converted to methane in older sediments, in which more labile OC fractions, such as OC from microalgal cells, have largely been remineralized already. Previous research in Lake Geneva revealed higher benthic CH<sub>4</sub> fluxes, but lower total mineralization rates of organic matter in deltaic sediments, compared to profundal sites with reduced riverine impact (Randlett et al., 2015). The observed differences imply that despite less efficient total remineralization that leads to elevated OC burial rates in deltaic sediments, high CH<sub>4</sub> production is sustained due to the high input of allochthonous OC (Sollberger et al., 2014).

Here we investigated relationships between methanogenesis rates and pathways, and the sources and degradation state of sedimentary organic matter in profundal and deltaic sediments of Lake Geneva. We combined methanogenic rate measurements by radiotracer incubations with <sup>14</sup>C-labeled bicarbonate and acetate with compositional (lipids, pyrolysis-GC/MS) and stable carbon isotopic analyses of organic carbon and CH<sub>4</sub>, and sedimentation rate measurements (based on Pb-210, Cs-137). Additional quantitative analyses of a methanogenic marker gene (*mcrA*) and analyses of methanogenic community structure (16S rRNA gene sequences) provided insights into the abundances and identities of in situ methanogenic populations. Based on this multi-disciplinary data set, we identified potential relationships between sediment OC sources and degradation status, rates, pathways, and the organisms involved in the microbial production of methane.

## **2. Material and methods**

### **2.1. Study sites**

Lake Geneva is the largest western European lake. The Rhone River, the main tributary to the lake in the northeastern part, has a catchment area of 5220 km<sup>2</sup> and accounts for about 68% of the total water discharge and large amounts of suspended sediment and fine-particle loading to the lake (Burrus et al., 1989). The Rhone River

inflow brings in large amounts of terrestrial OC, which is mostly deposited near the river mouth as an important contribution to deltaic sediments. On the other hand, sedimentation in the deeper part of the lake is usually dominated by phytoplankton-derived OC (Gallina et al., 2017).

## **2.2. Sample collection and processing**

Sediment cores were collected using a larger gravity corer (14 cm inner diameter) at a profundal site (46°25'54"N, 6°47'33"E, water depth: 240 m) and a smaller gravity corer (6.5 cm inner diameter) at a deltaic site (46°24'58"N, 6°51'34"E, water depth: 128 m) in August and December 2019, respectively. Profundal samples for different analyses were obtained from a single sediment core at 2-cm vertical resolution. Samples for the analysis of dissolved methane concentrations were collected on site with cut-off syringes through pre-drilled holes in the core liner covered with adhesive tape. Sediment samples of 2 cm<sup>3</sup> were fixed with 5 mL 10% NaOH in 120 mL serum bottles, which were capped immediately with thick butyl rubber stoppers and an aluminum crimp cap. Additionally, two replicate samples were taken from the same depth for methanogenesis rate measurements (described below). Sediment porewater was extracted with Rhizon samplers (Rhizosphere Research Products, Wageningen, Netherlands) connected to 20-mL syringes through predrilled small holes, with 2 cm distance between them. Porewater samples for DIC concentration measurements and stable carbon isotope analyses were stored in 4-mL glass vials without headspace at 4 °C. Separate porewater sample aliquots for the quantification of acetate and other volatile fatty acids were stored in combusted (450 °C for 5 h) glass vials at -20 °C until further analysis. The sediment core was then extruded in the lab and sectioned into 2 cm segments. Samples were taken from each segment and stored frozen (-20 °C) until further analysis for bulk parameters and lipid biomarkers. Using the gravity corer equipped with the smaller core liner, four sediment cores were obtained from the deltaic site. One core was used for methane concentration measurements, a second one for rate measurements (both at 2-cm resolution, sample collection as described above). The third core was used for porewater extraction in the lab using Rhizon samplers, and the last one was split open for the determination of porosity, analysis of bulk parameters and lipid biomarkers. An additional small-diameter sediment core was taken at the profundal site during the second sampling campaign for porosity analysis.

### 2.3. Rate measurements of methanogenesis using radiolabeled substrates

Methanogenesis rates (MGR) were determined using a radioisotope-based approach. We determined the modes of methane production and activity rates in incubation experiments with radio-labeled acetate and bicarbonate. At each depth, samples (2.5 cm<sup>3</sup>) were collected through pre-drilled holes using 3 mL cut-off plastic syringes, which were closed with rubber stoppers and stored at 4 °C. Upon arrival of the samples in the laboratory, ten microliters of anoxic <sup>14</sup>C-labeled bicarbonate (~16 kBq, Perkin-Elmer) or 2-<sup>14</sup>C-labeled (i.e., <sup>14</sup>C label in the methyl group) acetate solution (~18 kBq, Perkin-Elmer) were injected for the MGR measurements to determine CO<sub>2</sub> reduction (MGR<sub>DIC</sub>) and acetoclastic (MGR<sub>Ac</sub>) methanogenesis rates, respectively. Immediately after the tracer injection through the stoppers, all samples including killed controls (i.e., samples that were transferred to 10 mL 5% NaOH solution immediately after tracer injection) were incubated under an N<sub>2</sub> atmosphere at in situ temperature (4 °C) in the dark for 48 h.

To stop microbial activity in the incubations with <sup>14</sup>C-labeled substrates, samples were transferred into 120-mL serum bottles containing 10 mL aqueous NaOH (5% wt:wt), immediately crimp-sealed with butyl rubber stoppers and vigorously shaken. The <sup>14</sup>C activity in the different carbon pools was determined as previously described (Su et al., 2019). In brief, the headspace of a fixed sample is purged with air (30 mL min<sup>-1</sup> for 30 min) through a heated (850 °C) quartz tube filled with copper oxide, where the <sup>14</sup>CH<sub>4</sub> (product of methanogenesis during incubation) is combusted to <sup>14</sup>CO<sub>2</sub>. The <sup>14</sup>CO<sub>2</sub> is then captured in two sequential traps of scintillation vials (20 mL) containing 8 mL of 1:7 phenylethylamine and methoxyethanol. The cumulative radioactivity of both traps is then determined by liquid scintillation counting (2200CA Tri-Carb Liquid Scintillation Analyzer) after adding 8 mL of a scintillation cocktail (Ultima Gold, PerkinElmer) to each vial, and thorough mixing using a vortex-mixer. For incubations with bicarbonate, the residual <sup>14</sup>C-bicarbonate was measured as <sup>14</sup>CO<sub>2</sub>, released from the alkaline liquid phase after adding 2.5 mL of 32% HCl. The remaining radioactivity (possibly explained by inorganic carbon assimilation into biomass) was determined in a 1-mL aliquot of the acidified mixture (amended with 4 mL Ultima Gold) by liquid scintillation counting. Incubation bottles with <sup>14</sup>C-acetate were also acidified with 2.5 mL of 32% HCl after extraction of <sup>14</sup>CH<sub>4</sub>, and <sup>14</sup>CO<sub>2</sub> from microbial acetate oxidation was subsequently purged and trapped as described above. To determine the residual <sup>14</sup>C-acetate in the incubation vial, 1 mL of the acidified mixture was mixed with 4 mL

Ultima Gold for scintillation counting (Beulig et al., 2018). The control samples were processed in the same way as the incubated samples after the termination of incubation. The methanogenesis rates with DIC ( $\text{nmol cm}^{-3} \text{ d}^{-1}$ ) and acetate ( $\text{nmol cm}^{-3} \text{ d}^{-1}$ ) as substrates were calculated using Eq. 1 and Eq. 2, respectively, modified from a previous study (Beulig et al., 2018).

$$MGR_{DIC} = 1.08 \times \varphi \times [DIC] \times \frac{A_{CH_4}}{A_{CH_4} + A_{DIC} + A_R} \times t^{-1} \quad (1)$$

$$MGR_{Ac} = 1.08 \times \varphi \times [Ac] \times \frac{A_{CH_4}}{A_{CH_4} + A_{DIC} + A_{Ac}} \times t^{-1} \quad (2)$$

$[DIC]$  and  $[Ac]$  are concentrations of DIC and acetate in the sediment porewater, respectively.  $A_{CH_4}$  and  $A_{DIC}$  represent the activities of produced  $\text{CH}_4$  and DIC (i.e., residual DIC in bicarbonate-amended incubations, product DIC in acetate-amended incubations) at the end of the incubation (in CPM).  $A_R$  and  $A_{Ac}$  represent the remaining radioactivity of DIC-incubated samples (i.e., biomass and metabolic intermediates) and the residual  $^{14}\text{C}$ -acetate radioactivity (possibly also including a small fraction of  $^{14}\text{C}$  in metabolic intermediates and incorporated into biomass), respectively.  $\varphi$  is the porosity of the sediment samples. The factor 1.08 accounts for the isotopic fractionation of  $^{14}\text{C}$  (Hansen et al., 2001).  $t$  represents the incubation time in days. Measured  $^{14}\text{CH}_4$  activities in all incubation samples were blank-corrected by subtracting the  $^{14}\text{CH}_4$  activity measured in the killed control (typically close to background radioactivity) incubated with the same amounts of  $^{14}\text{C}$ -labeled substrates. The activities in the  $^{14}\text{CH}_4$  pool were considered zero if the blank-corrected value was negative.

## 2.4. Pore water methane and nutrient analyses

Methane concentrations were measured in the headspace of NaOH-preserved samples using a gas chromatograph (GC, Agilent 6890N) with a flame ionization detector, and helium as a carrier gas.  $\text{CH}_4$  concentrations in the wet sediments were then calculated based on the headspace-to-sample volume ratio. The C isotopic composition ( $^{13}\text{C}/^{12}\text{C}$ ) of methane was determined in the same samples using a pre-concentration unit (TraceGas, Micromass, UK) connected to an isotope ratio mass spectrometer (IRMS; GV Instruments, Isoprime). Stable C-isotope values are reported in the conventional  $\delta$  notation (in ‰) relative to the Vienna Pee Dee Belemnite standard (V-PDB), with a reproducibility of 0.5‰ based on replicate measurements of methane standards. A carbon analyzer (TOC-L, Shimadzu, Kyoto, Japan) was used to quantify

dissolved inorganic carbon (DIC) concentrations in sediment porewaters. Samples were manually injected into the DIC reaction vessel and measured with a non-dispersive infrared detector (NDIR) after acidification and volatilization to CO<sub>2</sub>. To determine the carbon isotopic composition of DIC, a porewater aliquot of 1-2 mL was introduced into a He-purged exetainer (Labco Ltd) and acidified with ~200 µL 85% H<sub>3</sub>PO<sub>4</sub>. After 2 h equilibration at 37 °C, the CO<sub>2</sub> released from the aqueous phase was subsequently analyzed using a preparation system (MultiFlow, Isoprime) coupled to an IRMS (Micromass, Isoprime). The standard deviation for replicate measurements of samples and standards was < 0.2‰. The apparent carbon isotope fractionation factor ( $\alpha_c$ ) during methanogenesis was estimated using  $\delta^{13}\text{C}$  values of CH<sub>4</sub> and DIC (Eq. 3).

$$\alpha_c = \frac{1000 + \delta^{13}\text{C-DIC}}{1000 + \delta^{13}\text{C-CH}_4} \quad (3)$$

Values of  $\alpha_c$  greater than 1.065 were interpreted to indicate a predominance of CO<sub>2</sub> reduction over acetoclastic methanogenesis (Conrad, 2005). Porewater samples for acetate and other volatile fatty acids were analyzed with a two-dimensional ion chromatography (2D IC), as described previously (Glombitza et al., 2014), with modifications reported in (Schaedler et al., 2018). Samples were filtered through pre-washed (10 mL Ultrapure Type I water) disposable syringe filters (Acrodisc® IC grade, 0.2 µm pore size, 13 mm diameter). The first 0.5 mL sample after filtration was discarded before collecting the samples for 2D IC analysis. We used a dual Dionex ICS6000 instrument (Thermo Scientific) equipped with a Dionex AS24 column (2 mm diameter) for the first dimension, and a Dionex AS11HC column (2 mm diameter) for the second dimension. Quantification was done from the conductivity detector signal with a series of 5 external standards between 0.5 and 100 µM.

## 2.5. Bulk sediment analyses

The total organic carbon (TOC) contents of sediment samples were determined by the difference between total carbon and total inorganic carbon. Samples for total carbon were measured with an Elementar Vario Pyro Cube CN elemental analyser (Elementar, Germany), and samples for total inorganic carbon were analysed by coulometry using a UIC CM5015 coulometer (Joliet, IL, USA). Sediment cores were dated by gamma spectrometry using <sup>137</sup>Cs on freeze-dried and ground sediment for the determination of sedimentation rates, as described previously (Randlett et al., 2015). The  $\delta^{13}\text{C}$ -TOC was determined on decalcified samples (Schubert and Nielsen, 2000). Briefly, freeze-dried



and homogenized samples were treated with 5 mL 10% HCl in 15 mL Falcon tubes overnight. After centrifugation, the supernatant was discarded, and the solid phase was washed/centrifuged three times with 5 mL MilliQ water. Samples were dried at 50 °C for 48 h prior to analysis. The  $\delta^{13}\text{C}$ -TOC was then assessed by elemental analysis-isotope ratio mass spectrometry (EA, Pyro Cube, Elementar and IRMS, Isoprime, UK). The reproducibility based on replicate measurements of standards and samples was better than 0.2‰.

## **2.6. Pyrolysis gas chromatography-mass spectrometry**

The sedimentary organic matter composition was characterized at the molecular level using a pyrolyzer equipped with an autosampler (EGA/PY-3030D and AS-1020E, FrontierLabs, Japan) connected to a gas chromatograph (Trace 1310, Thermo Scientific) and a mass spectrometer (ISQ 7000, Thermo Scientific), following the optimized method (Tolu et al., 2015). Depending on the sample, an aliquot of 2-3 mg of dry sediment was pyrolyzed at 450°C. A data-processing pipeline, including chromatogram smoothing, alignment background correction and multivariate curve resolution by alternate regression was used to automatically detect and integrate the peaks and extract their mass spectra under “R” computational environment (R Core Team, 2014). To optimize the number of detected peaks, data processing was performed independently for the sediments from the deltaic site (DS) and the profundal site (PS). Individual peaks were identified using “NIST MS Search 2” software which includes the library “NIST/EPA/NIH 2011”, complemented by spectra from published studies. The relative abundances of these identified pyrolytic organic compounds (Table S2) were calculated for each sample by normalization to the sum of their peak areas set at 100%.

## **2.7. Lipid extraction, separation, and quantification**

At both sites, sediment samples from five depths (1, 5, 11, 19, and 29 cm) were selected based on redox conditions (1 cm: oxic/suboxic; all others anoxic), organic carbon content, and methanogenesis rates (the latter two variables had peak value in the deeper layers), then lyophilized and homogenized for subsequent lipid extraction. Prior to extraction, an internal standard mix (5 $\alpha$ -androstane, 3-eicosanone, n-C19:0 fatty acid and n-C19 alkanol) was added to each sample for the quantification of single biomarkers. Lipids were extracted in 20 mL of 7:3 Dichloromethane/Methanol

(DCM/MeOH) in a Microwave Reaction System (SolvPro, Anton Paar, Graz, Austria), as described previously (Ladd et al., 2018). Total lipid extracts (TLEs) were obtained by successively rinsing the samples with DCM after centrifugation, and then concentrated using a Multivapor P-6 (Büchi Labortechnik AG, Switzerland). TLEs were further evaporated to dryness, and saponified in 3 mL methanolic KOH-solution (~1 N) at 80 °C for 3 h. Neutral compounds were extracted by liquid-liquid extraction using hexane, fatty acids (FAs) were then extracted from the remaining aqueous phase with hexane after acidification (pH < 2). The fatty acid fraction was treated using 1 mL of BF<sub>3</sub> in methanol (14% v/v, Sigma Aldrich) at 80 °C for 2 h, and converted to fatty acid methyl esters (FAMES). Neutral compounds were further separated into four different fractions using 500 mg/6mL pre-packed Si gel columns (filling quantity/volume, Biotage, Uppsala, Sweden). Briefly, the neutral fraction was dissolved in 4 mL hexane and transferred onto the column, followed by 4 mL hexane/DCM (2:1 v/v), then 4 mL DCM/MeOH (19:1 v/v) and finally 4 mL MeOH, with the elution of hydrocarbon, ketone, alcohol and remaining polar compounds, respectively. The alcohol fraction was acetylated in 25 µL acetic anhydride and 200 µL pyridine at 70 °C for 30 min.

All fractions were quantified using a gas chromatograph equipped with a flame ionization detector (GC-FID) (GC-2010 Plus, Shimadzu, Japan). Samples were injected onto an InertCap 5MS/NP column (0.25 mm × 30 m × 0.25 µm, GL Sciences, Japan) using an AOC-20i autosampler (Shimadzu) through a split/splitless injector operated in splitless mode at 280 °C. The column was heated from 70 °C to 130 °C at 20 °C min<sup>-1</sup>, then to 320 °C at 4 °C min<sup>-1</sup>, and held at 320 °C for 20 min. FAMES were identified by comparing their retention times to those of laboratory standards (i.e., a fatty acid methyl ester mix and bacterial acid methyl ester from Supelco, reference no. 47885-U and 47080-U, respectively), and were quantified by normalization to the internal n-C19:0 fatty acid standard. Identification of hydrocarbons was performed by comparing their retention times to those of an external standard containing C14 to C40 n-alkanes (Sigma-Aldrich). The alcohols were characterized using a gas chromatography-mass spectrometer (GC-MS, QP2020, Shimadzu, Japan) under identical chromatographic conditions. Acquired mass spectra were identified through comparison with published data.

## **2.8. Compound-specific stable carbon isotope analysis**

The stable carbon isotope composition of FAMES, n-alkanes and alcohols was determined by gas chromatography-isotope ratio mass spectrometry (GC-IRMS), using a Delta V Advantage IRMS (Thermo Scientific) with a ConFlow IV (Thermo Scientific). Samples were injected with a TriPlus RSH autosampler to a PTV inlet operated in splitless mode at 280 °C on a GC-1310 gas chromatograph (Thermo Scientific, Bremen, Germany). The GC was equipped with a 30 m DB-5MS fused silica capillary column (0.25 mm i.d., 0.25 µm film thickness). The GC oven was heated from 80 °C to 215 °C at 15 °C min<sup>-1</sup>, then to 320 °C at 5 °C min<sup>-1</sup>, and held at 320 °C for 10 min. Column effluent was combusted at 1020 °C. Compound-specific δ<sup>13</sup>C values were reported relative to the V-PDB scale, and calibrated externally using known δ<sup>13</sup>C values of an alkane mixture (n-C<sub>17</sub>, 19, 21, 23, 25, 28 and 34, Arndt Schimmelmann, Indiana University, USA), which were run at the beginning and the end of each sequence, as well as after every 6th sample injection. The standard deviation for replicate measurements for these standards averaged 0.4‰, with the average offset from their known values of less than 0.5‰. The isotopic values of FAMES and acetylated alcohols were additionally corrected for the introduction of carbon atoms during the derivatization step.

## **2.9. DNA extraction, PCR amplification, Illumina sequencing and data analysis**

DNA was extracted from selected sediment samples of Lake Geneva, where both high and low methanogenic activities were detected (DS: 11, 19, 21 and 27 cm; PS: 5, 11, 19, and 29 cm), using FastDNA SPIN Kit for Soils (MP Biomedicals) following the manufacturer's instructions. A two-step PCR approach was applied to prepare the library for Illumina sequencing at the Genomics Facility Basel, as described in detail previously (Su et al., 2020, 2023). PCR was performed using universal primers 515F-Y and 926R targeting the V4 and V5 regions of the 16S rRNA gene. These primers cover the majority (~84.7%) of the 16S rRNA gene sequences of methanogenic archaea and are well-suited for assessing community structures of methanogens in environmental samples (Table S4). Data were then analyzed with Phyloseq (McMurdie and Holmes, 2013) in the R environment (R Core Team, 2014). Raw sequence data were deposited at NCBI Short Read Archive under the Bioproject ID PRJNA736863 with accession numbers from SAMN19667760 to SAMN19667767.

## **2.10. Quantitative PCR (qPCR)**

The abundance of methanogens in Geneva sediments was determined by qPCR with the primer set mcrIRD and 2  $\mu$ L DNA as template (Lever and Teske, 2015). qPCR reactions of all DNA samples were performed using the SensiFAST SYBR No-ROX Kit (Bioline) on a Mic (Magnetic Induction Cyclor) real time PCR machine (Bio Molecular Systems, Inc). An initial denaturing step of 95 °C for 3 min was followed by 40 cycles of 5 s at 95 °C, 10 s at 56 °C, and 22 s at 72 °C. The specificity of the amplification was assessed by examining the melting curves from 72 °C to 95 °C. The calibration curve was generated using a serial of 10-fold dilutions of pGEM-T Easy plasmid DNA (Promega, USA) carrying a single copy of the target gene (mcrIRD-F/mcrIRD-R). The number of gene copies in plasmid DNA was calculated using the equation reported previously (Ritalahti et al., 2006). We further compared the absolute gene copy numbers of *mcrA* between the two sites using the Wilcoxon signed-rank test ('wilcox.test'), implemented in the R package 'stats' (R Core Team, 2014).

### 3. Results

#### 3.1. Sediment geochemistry at the two study sites

The two sites displayed different hydro- and geochemical characteristics (Fig. 1 and Table S1 and Fig. S1). Dating of the sediments revealed that the deltaic site had a slightly higher sedimentation rate (0.58 cm yr<sup>-1</sup>) than the profundal site (0.43 cm yr<sup>-1</sup>). At the deltaic site (DS), two distinct peaks in methane concentration (~7 mM) were observed at 9 and 23 cm, respectively (Fig. 1A). At the profundal site (PS), concentrations of CH<sub>4</sub> increased with depth and remained relatively constant at ~4 mM below 15 cm (Fig. 1E). At both sites, the pore water concentrations of dissolved inorganic carbon (DIC) increased with depth, and considerable amounts accumulated in the sediment pore water. The depth-integrated DIC concentrations in the top 30 cm were 1964 mmol m<sup>-2</sup> at PS and 3490 mmol m<sup>-2</sup> at DS, however, based on the sedimentation over the past 50 years, the depth-integrated DIC concentrations were 1302 mmol m<sup>-2</sup> at PS (21 cm) and 3490 mmol m<sup>-2</sup> at DS (29 cm). Acetate, as a potential methanogenic substrate, showed concentration maxima of 25.9  $\mu$ M (DS) and 3.8  $\mu$ M (PS) close to the sediment surface. The methane  $\delta^{13}\text{C}$  values decreased with depth in both deltaic sediments (from -64.9‰ to -72.2‰, Fig. 1B) and profundal sediments (from -72.7‰ to -74.6‰, Fig. 1F). Overall, the observed methane carbon isotope values at both sites fall within a range that is typical for biogenic production (Whiticar, 1999).

Vertical profiles of  $\delta^{13}\text{C}$ -DIC show similar pattern at the two sites, with the lowest values of -5.5‰ at 5 cm at DS (Fig. 1B) and -5.2‰ at 3 cm at PS (Fig. 1F). At PS, TOC concentrations increase slightly with depth, with the mean content almost doubled compared to DS (Fig. 1C and G, Table S1). With respect to its stable carbon isotope composition,  $\delta^{13}\text{C}$ -TOC increased slightly with depth at PS, from -28‰ in surficial sediments to -26‰ below 7 cm whereas  $\delta^{13}\text{C}$ -TOC values remained relatively constant at DS throughout the sampled sediment column (~ -26‰). The elemental C/N ratios in the sediments of DS show a very high variability with depth, and range from 6.7 to 16.8, with a mean value of 10.7 (Fig. 1D and Table S1), while the values at PS are lower and less variant along the sediment core ( $7.9 \pm 0.3$ , Fig. 1 H).

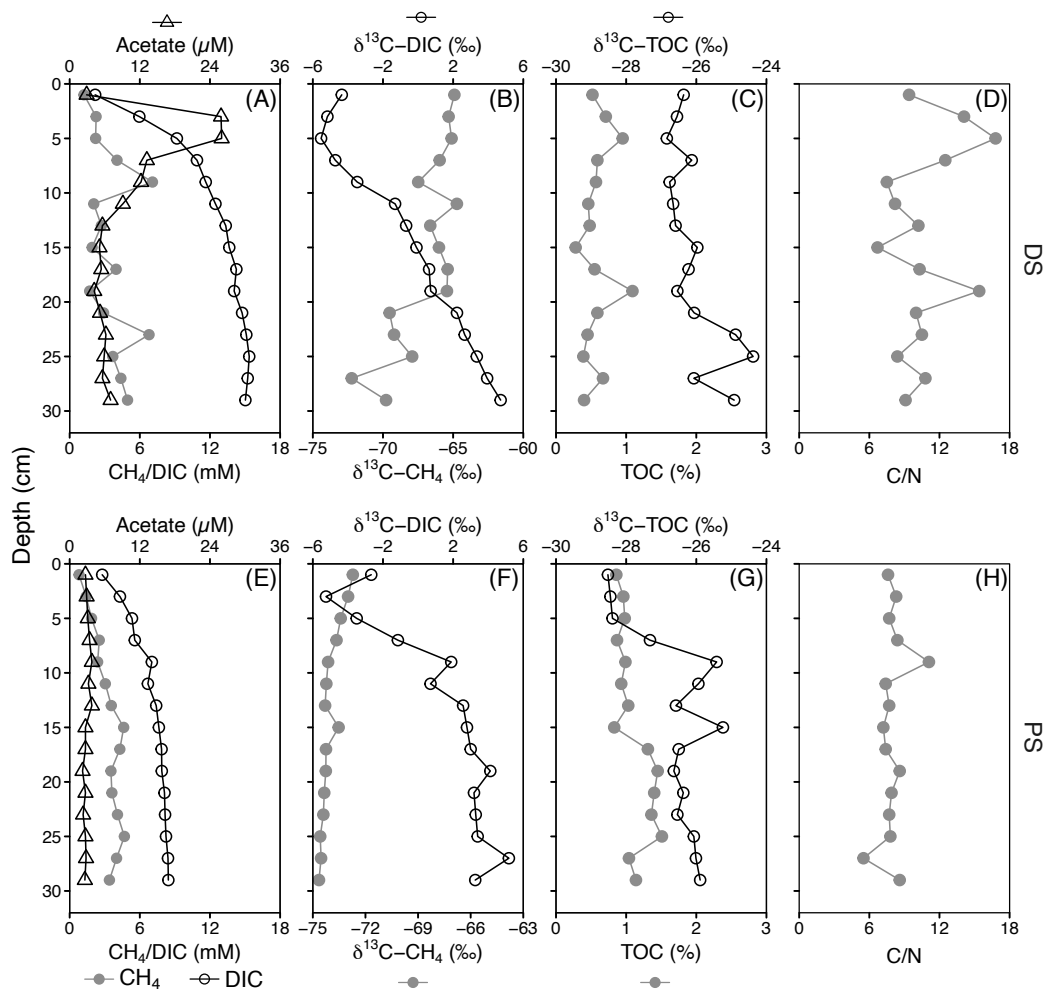


Figure 1. Sediment geochemistry as function of depth at a deltaic site (DS, A-D) and a profundal site (PS, E-H) in Lake Geneva. (A, E) Profiles of dissolved methane, dissolved inorganic carbon (DIC) and acetate concentrations. (B, F) Stable carbon isotopic signatures ( $\delta^{13}\text{C}$ ) of  $\text{CH}_4$  and DIC (in ‰ vs. V-PDB). (C, G) Concentrations of

total organic carbon (TOC, % of dry weight) and its carbon isotopic composition (in ‰ vs. V-PDB). (D, H) Molar ratios of total organic carbon to total nitrogen (C/N).

### 3.2. Composition of sedimentary organic matter

To investigate the molecular composition of sedimentary organic matter at the two different sites, sediment samples were further analyzed using Py-GC/MS. We identified a total of 65 individual organic compounds (Table S2), which can be classified into the following compound groups: carbohydrates, N-compounds, *n*-alkenes, *n*-alkanes, phenols, lignin oligomers, and (poly)aromatics. Both carbohydrates and N-compounds were the most abundant organic compound groups among the pyrolysis products, with no statistical difference between DS and PS (Fig. 2 A and B). At both sites, the carbohydrates consisted mainly of compounds such as butenal, methylfuraldehyde and furanone, and N-compounds were dominated by pyrrole, pyridine, methyl-pyrrole and methyl-pyridine (Table S2), which are indicative of degraded products of carbohydrates and proteins (Schellekens et al., 2009; Tolu et al., 2017). Most strikingly, sediments at DS displayed significantly higher relative abundances of lignin ( $p < 0.05$ ) and phenols ( $p < 0.01$ ) compared to profundal sediments (Fig. 3D and E). In addition, we observed significantly higher relative abundances of *n*-alkenes at PS (Fig. 3C). This group contains monounsaturated short-chain *n*-C<sub>15</sub> to *n*-C<sub>18</sub> (Table S2), which were the most abundant organic compounds among the *n*-alkenes.

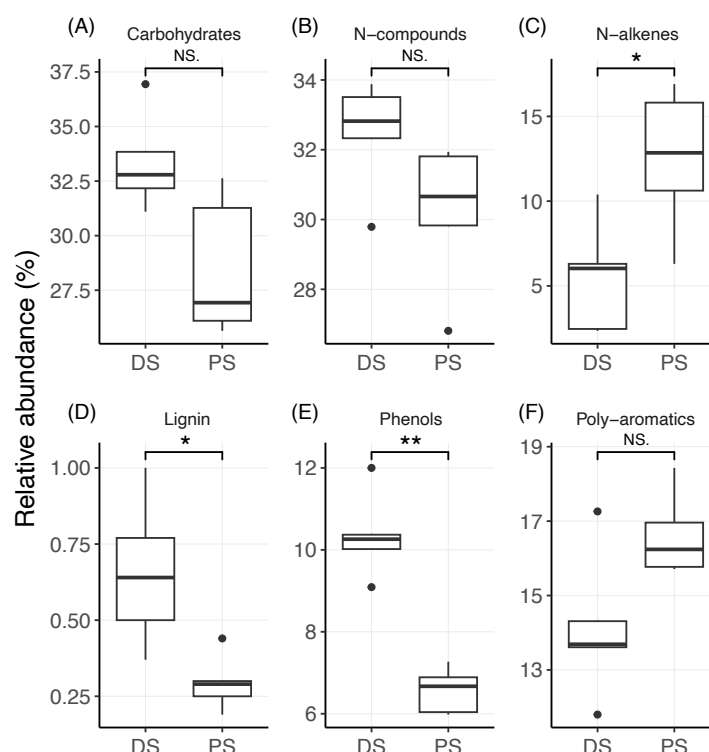


Figure 2. Relative abundances (in %) of different biochemical classes of organic compounds in sediments at the deltaic (DS) and profundal site (PS) of Lake Geneva. (A) Carbohydrates, (B) N-compounds, (C) N-alkenes, (D) Lignin, (E) Phenols and (F) Poly-aromatics. Statistical differences of compound abundances between the two sites were determined with the Wilcoxon signed-rank test. Significance levels are: \*\*  $p < 0.01$ ; \*  $p < 0.05$ ; NS. no significant differences between the two sites ( $p > 0.05$ ).

### 3.3. Lipid concentration, distribution, and stable carbon isotopic signature

Typical lipid biomarkers derived from aquatic phytoplankton (e.g., short-chain fatty acids) and terrestrial plants (e.g., long-chain n-alkanes) were present in both profundal and deltaic sediments, yet concentrations of some of these biomarkers were strikingly different between the two sites, as well as between different depths within the same site (Fig. 3 and Table S3). Among the fatty acids,  $n\text{-C}_{16:0}$  was by far the most abundant in all measured samples, with a slight increase in  $\delta^{13}\text{C}$  values with depth at both sites. At DS, the unsaturated fatty acids  $n\text{-C}_{16:1\omega7}$  was the most abundant monounsaturated fatty acids with the highest concentration observed at 11cm. At PS,  $n\text{-C}_{16:1}$  ( $\omega7$  and  $\omega5$ ) and  $n\text{-C}_{18:1}$  ( $\omega9$  and  $\omega7$ ) decreased in concentration with depth and were two to four times more abundant in the upper sediment layers (0-2 cm, 4-6 and 10-12 cm) than in the lower parts (18-20 and 28-30 cm). The short-chain fatty acids

462 were generally depleted in  $^{13}\text{C}$ , with stronger  $^{13}\text{C}$ -depletions observed in surface  
463 sediments, particularly for the unsaturated fatty acids  $n\text{-C}_{16:1\omega5}$  at PS.

464 In contrast to short-chain fatty acids,  $\text{C}_{24:0}$  was most abundant among the long-  
465 chain fatty acids (i.e.,  $\text{C}_{24:0}$ ,  $\text{C}_{26:0}$  and  $\text{C}_{28:0}$ ), with relatively higher concentrations found  
466 in profundal sediments. Most strikingly, an apparent increase in the concentrations of  
467 these long-chain fatty acids was observed in the sediments of PS, with consistently high  
468 concentrations in the lower parts (10-30 cm). Meanwhile, the  $\delta^{13}\text{C}$  values of these  
469 compounds decreased dramatically with depth. By comparison, concentrations of long-  
470 chain fatty acids at DS were variable at different sediment depths, but their  $\delta^{13}\text{C}$  values  
471 remained relatively constant (e.g.,  $\text{C}_{28:0}$ , Fig. 3B) and showed less variability with depth  
472 compared with PS (e.g.,  $\text{C}_{24:0}$  and  $\text{C}_{26:0}$ ). Although the concentrations of long-chain n-  
473 alkanes at DS were twice as high as those at PS, their  $\delta^{13}\text{C}$  values (particularly for  $\text{C}_{29}$ ,  
474  $\text{C}_{31}$  and  $\text{C}_{33}$ ) were very similar at the two sites (Fig. 3B).



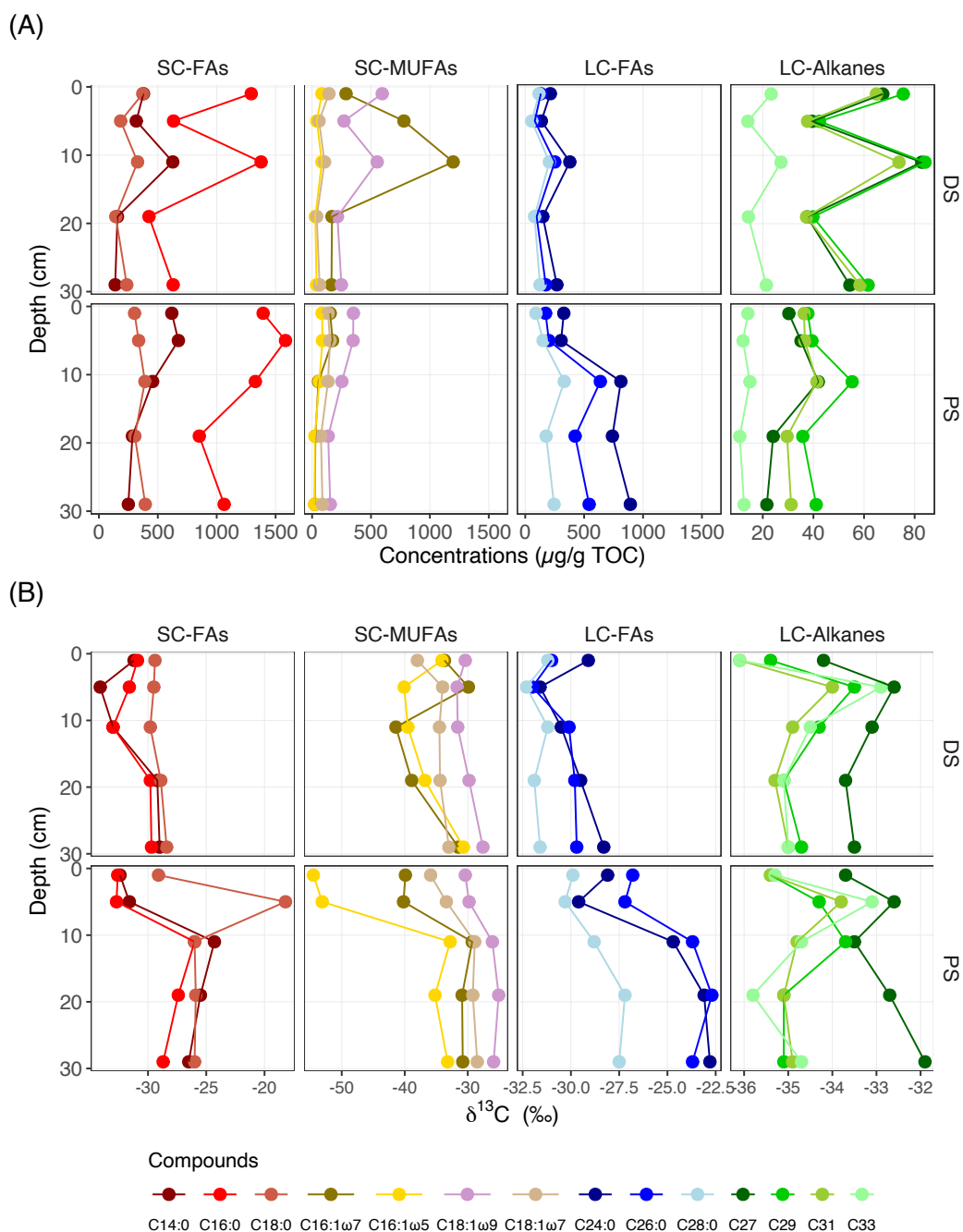


Figure 3. Vertical distribution of specific fatty acids and n-alkanes in deltaic (DS) and profundal (PS) sediments of Lake Geneva. (A) Concentrations (expressed as  $\mu\text{g}$  lipid  $\text{g}^{-1}$  TOC), and (B) compound-specific  $\delta^{13}\text{C}$  values (in ‰ vs. V-PDB). SC-FAs, short-chain fatty acids ( $\text{C}_{14:0} + \text{C}_{16:0} + \text{C}_{18:0}$ ); SC-MUFAs, short-chain monounsaturated fatty acids ( $\text{C}_{16:1}$  and  $\text{C}_{18:1}$ ); LC-FAs, long-chain fatty acids ( $\text{C}_{24:0} + \text{C}_{26:0} + \text{C}_{28:0}$ ); LC-Alkanes, long-chain n-alkanes ( $\text{C}_{27} + \text{C}_{29} + \text{C}_{31} + \text{C}_{33}$ ).

### 3.4. Relative importance of methanogenic pathways

Methane production through CO<sub>2</sub> reduction was observed at both sites and at all depths. At the deltaic site, highest activity of CO<sub>2</sub> reduction methanogenesis was found at the lower part of the sediment core (19-29 cm), while in the profundal sediment, maximum rates of methanogenesis via this pathway were detected within the upper sediments at depths between 7 and 17 cm (Fig. 4B and E, Table S1). In contrast, the rates of methane production via acetate fermentation (i.e., acetoclastic methanogenesis) were low, with maxima of 2.8 and 1.0 nmol cm<sup>-3</sup> d<sup>-1</sup> observed at 3 cm (PS) and 7 cm (DS), respectively. The areal methanogenesis rates by CO<sub>2</sub> reduction within the top 30 cm, at both sites, were two orders of magnitude higher than acetoclastic methanogenesis rates (Table S1). Acetate oxidation activity was very low at both PS and DS, with the depth-integrated (0-30 cm) rates of 0.1 and 0.2 mmol m<sup>-2</sup> d<sup>-1</sup>, respectively (Table S1). At both sites, the fractionation factor  $\alpha_c$ , which is approximated based on the difference between the measured  $\delta^{13}\text{C}$ -DIC and  $\delta^{13}\text{C}$ -CH<sub>4</sub> values, increased with depth (Fig. 4F), ranging from 1.064-1.071 (DS) and 1.073-1.084 (PS).

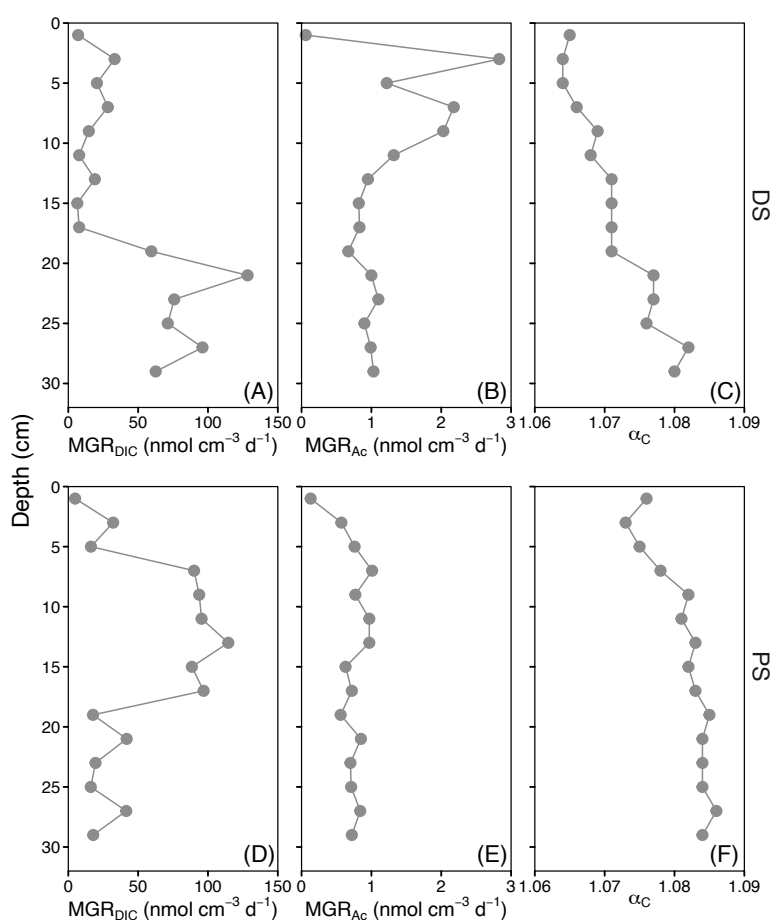


Figure 4. Depth profiles of (A, D) CO<sub>2</sub> reduction methanogenesis rates (MGR<sub>DIC</sub>), (B, E) acetoclastic methanogenesis rates (MGR<sub>Ac</sub>), and (C, F) apparent fractionation factor  $\alpha_C$  in sediments of deltaic (DS) and profundal site (PS) in Lake Geneva.

### 3.5. Abundance and diversity of methanogenic archaea

On average, gene copy numbers of the methyl coenzyme M reductase gene (*mcrA*) in the deltaic sediments of Lake Geneva were significantly higher than those in the profundal sediments ( $p < 0.05$ ; Fig. 5A). At both sites, *Methanoregula* and *Methanothrix* dominated the methanogenic guild, followed by *Methanosarcina* and *Methanobacterium* (Fig. 5B). Within the methanogenic community, the mean relative abundances of *Methanothrix* and *Methanosarcina* were both higher at DS than those at PS. By comparison, *Methanoregula* was the most abundant genus in the methanogenic community at PS.

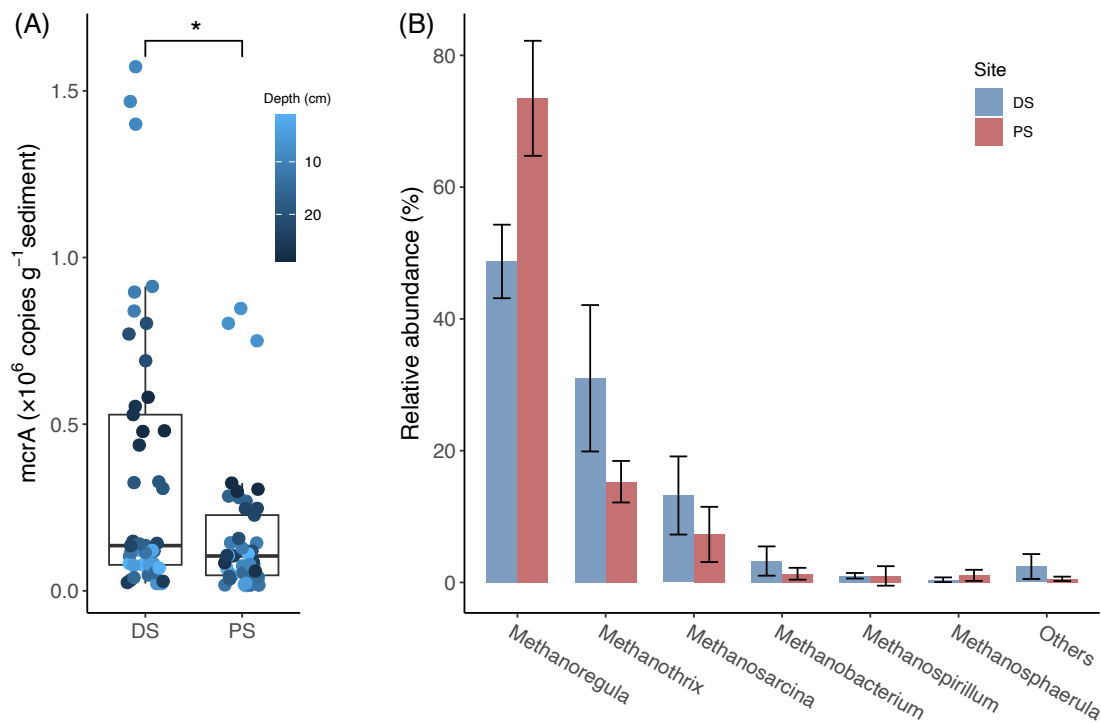


Figure 5. Abundance and diversity of methanogens at the deltaic (DS) and the profundal site (PS) in Lake Geneva. (A) Absolute abundances of the *mcrA* gene encoding the  $\alpha$ -subunit of the methyl-coenzyme M reductase. Statistical difference between the two sites was determined with the Wilcoxon signed-rank test and asterisk denotes significance level (\*:  $p < 0.05$ ). (B) Mean relative abundances of different methanogenic

groups (% of the total methanogens). Data are based on read abundances of 16S rRNA gene sequences.

### **3.6. Correlation analysis between geochemical parameters, methane production rates, and microbial communities**

The alpha diversity measures indicate that the community structure of microorganisms in the sediments at DS were more diverse than at PS (Fig. S2). Principal coordinate analysis (PCoA) revealed significantly different microbial community compositions at the two investigated sites, as indicated by the clear separation of the data by the first principal coordinate, explaining 50.8% and 44.5% of the observed variance for archaea and bacteria, respectively (Fig. S3). For both archaeal and bacterial communities, PCoA plots show a very close aggregation of the deep sediment samples at PS (17, 23 and 29 cm), indicating that their community structures are highly similar. Conversely, there is quite some variance among the samples at the more dynamic deltaic site DS, with its variable deposition history. The measured rates of both CO<sub>2</sub> reduction and acetoclastic methanogenesis tend to be higher in sediment samples harboring a more diverse microbial community (Fig. S4), but the relation is weak and particularly for acetoclastic methanogenesis not significant. Pearson correlation analysis between methane production rates and environmental parameters show that methane production rates from both MGR<sub>DIC</sub> and MGR<sub>Ac</sub> was positively but not significantly correlated with the concentration of short-chain n-alkanes (correlation coefficients of 0.46 and 0.51 for MGR<sub>DIC</sub> and MGR<sub>Ac</sub>, respectively, Fig. S5).  $\delta^{13}\text{C-CH}_4$  values showed a positive correlation with the abundance of carbohydrates, lignin, and long-chain n-alkanes, and significant negative correlation with the abundance of long-chain fatty acids and total organic carbon. C/N ratios were negatively correlated with the concentrations of both short-chain and long-chain fatty acids (Fig. S5).

## **4. Discussion**

Our results indicate a dominance of methane production by CO<sub>2</sub> reduction in both profundal and deltaic sediments of Lake Geneva. This inference is supported by radiotracer measurements, the observed apparent fractionation factors, and methanogenic community analyses, which revealed members of CO<sub>2</sub>-reducing *Methanoregula* as the dominant group of methanogens. Thus, CO<sub>2</sub> reduction was

observed as the primary MGR process both in sediments at PS, which predominantly contained diagenetically altered phytoplankton-derived OC, and sediments at DS characterized by variable sources of aquatic and terrestrial OC. We conclude, therefore, that the dominant pathway of methanogenesis does not primarily depend on the chemical composition of sedimentary organic matter. Other factors that affect production rates of different electron donors (e.g., H<sub>2</sub>, acetate) could play a more important role, and will be discussed below.

#### **4.1. Difference in organic carbon sources and diagenetic alteration**

The deltaic sediments in this study displayed a strikingly large range of C/N ratios (6.7-16.8), whereas C/N ratios of profundal samples remained relatively constant throughout the sediment core ( $7.9 \pm 0.3$ ). Fresh organic matter from lacustrine phytoplankton, which is protein- rich (Parsons et al., 1961), typically has low C/N ratios of 6-9 (Meyers and Ishiwatari, 1993). In contrast, bulk sediment containing large portions of terrestrial vascular plants often displays much higher C/N ratios, sometimes at least three times greater, due to its high content of high-carbon structural components and refractory organics such as lignin (Hedges et al., 1986). A comparison of carbon isotope and bulk C/N values to data from previous studies (Lamb et al., 2006) confirmed the presence of both aquatic and terrestrial sources in the deltaic sediments, and the dominance of organic matter of autochthonous origin (e.g., algal biomass) at PS (Fig. 6). At DS, variable microbial community structures and significant changes in C/N ratios with depth reflect a highly variable depositional history, indicating differing origins of sedimentary organic matter. Specifically, peak C/N ratios of 16.8 at 5 cm and 15.4 at 19 cm were likely derived from terrestrial organic matter in these intercalated layers, while relatively lower ratios (~10) at other depths suggest a mixture of aquatic and terrestrial sources. Even lower values (~7) in some deltaic sediment layers may indicate predominantly autochthonous deposition of phytoplankton particles.

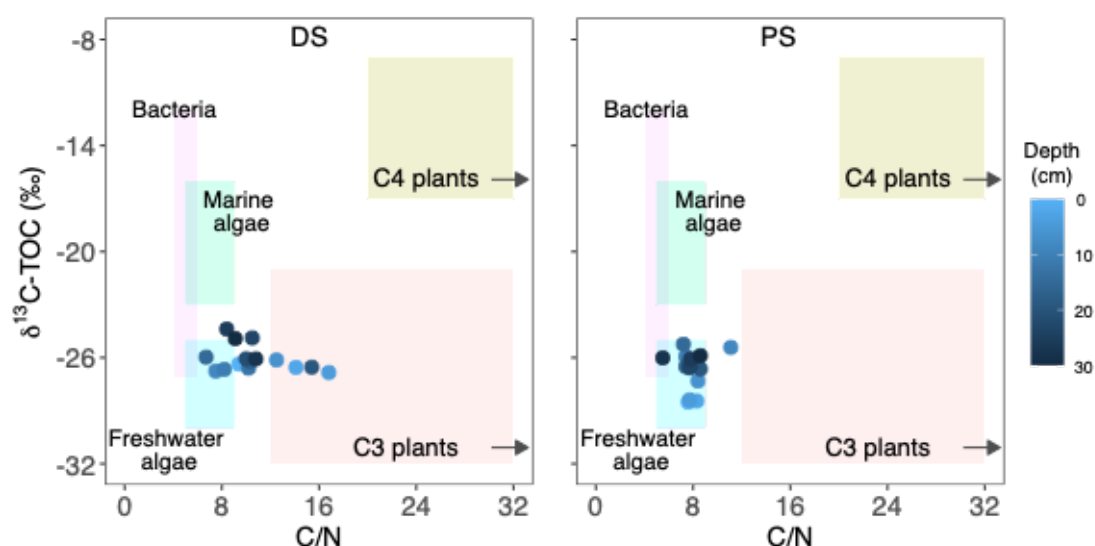


Figure 6. Comparison of  $\delta^{13}\text{C}$  and bulk C/N values of Lake Geneva sediments from the deltaic (DS, left) and profundal site (PS, right) to elemental and isotopic indicators of bulk organic matter produced by bacteria, marine and freshwater algae, as well as terrestrial C3 and C4 plants (Lamb et al., 2006).

Indeed, at both sites, sediments contained OC from aquatic biomass, as verified by the short-chain fatty acids, indicative of freshwater algae (Cranwell, 1976), and/or in situ production by bacteria (Volkman et al., 1998). However, contrary to the findings from the combined carbon isotope and bulk C/N ratios, both lignin/phenols (Fig. 2) and long-chain n-alkanes (Fig. 3A) derived from terrestrial plants were detected in profundal sediments, although the concentrations of these compounds were lower at PS than at DS. Long-chain fatty acids (i.e.,  $\text{C}_{24:0}$  and  $\text{C}_{26:0}$ ), which are typically assumed to originate from terrestrial plant waxes (Cranwell, 1974), make up a proportionally more important fraction of lipids in deeper sediment layers, particularly below 5 cm depth. However, the distinct carbon isotope compositions of these long-chain fatty acids between the two sites (Fig. 3B and Table S3,  $\delta^{13}\text{C}$  on average  $\sim 7\text{‰}$  lower at DS than at PS) suggest different OC sources.

Indeed, Chikaraishi et al. (2004) reported that long-chain fatty acids (i.e.,  $\text{C}_{24:0}$  and  $\text{C}_{26:0}$ ) have  $\delta^{13}\text{C}$  values of  $-36.3 \pm 2.6\text{‰}$  for a variety of terrestrial vascular plants, whereas the  $\delta^{13}\text{C}$  for aquatic plants is significantly less negative ( $-25.5 \pm 0.9\text{‰}$ ). At PS,  $\delta^{13}\text{C}$  values for  $\text{C}_{24:0}$  and  $\text{C}_{26:0}$  fatty acids (below 5 cm depth) were close to those indicative of freshwater aquatic plants (Chikaraishi et al., 2004). Previous studies have shown that both aquatic macrophytes and microalgae may represent potential sources

of long-chain fatty acids (Ficken et al., 2000; Volkman et al., 1998). However, it seems somewhat contradictory to conclude that long-chain fatty acids were primarily derived from aquatic vascular plants, simply because the observed C/N ratios at PS were too low. Indeed, microalgae such as diatoms were estimated to contribute from 30-80% of the C<sub>24:0</sub> to C<sub>28:0</sub> fatty acid pool in intertidal sandy sediment (Volkman et al., 1980). Thus, the long-chain fatty acids observed in the profundal sediments may also have been derived from microalgae (Volkman et al., 1998). This, in turn, could explain why TOC was more depleted in <sup>13</sup>C in the surface sediments at PS, which does not necessarily indicate the origins of terrestrial plants (Cloern et al., 2002).

The carbon isotopic composition of long-chain n-alkanes (i.e., C<sub>27-31</sub>), characteristic for land-derived organic matter (Chikaraishi et al., 2004), was almost identical between PS and DS (Fig. 3B, ranging from -35‰ to -33‰), suggesting a similar terrestrial source. At DS, if long-chain n-alkanes and long-chain fatty acids were derived from the same terrestrial source, they should have similar C-isotopic values. However, the slightly lower  $\delta^{13}\text{C}$  values of long-chain fatty acids at DS (on average, -30‰) imply a mixture of both aquatic and terrestrial sources, which is consistent with the C/N ratios observed at this site.

Turning to other OM biomarkers, phytol concentrations were considerably higher at PS (with no clear depth trend) compared to DS, whereas no clear difference in cholesterol concentrations was observed between the sites (with depth-dependent concentration decrease at both sites). For brassicasterol, there seems to be a clear depth-related decrease at both sites, with slightly higher concentrations in surface sediments (0-2 and 4-6 cm) at PS compared to DS. Phytol, a side chain of chlorophyll, can originate from both phytoplankton and terrestrial plants (Shi et al., 2001). Due to its rapid degradation under intense-light and oxic conditions in terrestrial environments, terrestrially derived phytol (or chlorophyll) is generally of minor importance in aquatic sediments (Meyers and Takeuchi, 1981), so it can be assumed that most of the sedimentary phytol is derived from aquatic sources (Ladd et al., 2018). As for cholestanol and brassicasterol (Table S3), the former can originate from both zooplankton and phytoplankton (Bechtel and Schubert, 2009), while the latter is a lipid biomarker mainly derived from phytoplankton in aquatic sediments (Volkman, 1986). Hence, based on at least two of the biomarkers presented here, we have putative evidence for a shift towards more autochthonous OM at the profundal site, as could be expected.

## 4.2. Methanogenesis is mainly driven by CO<sub>2</sub> reduction

Our rate measurements using trace <sup>14</sup>C-labelled substrates clearly showed that CO<sub>2</sub> reduction played a dominant role in methane formation in both the PS and DS sediments, compared to acetoclastic methanogenesis. As we did not measure rates of methylotrophic methanogenesis, we are unable to determine the relative importance of this pathway. However, since we neither detected common methylated compounds such as methanol in the sediment porewater, nor methanogens that exclusively perform methylotrophic methanogenesis at any of the studied sites, we argue that this pathway is likely of a minor importance with regards to its contribution to the overall methane production at these sites. Indeed, H<sub>2</sub>/CO<sub>2</sub> and acetate are usually the main substrates in freshwater environments (Lyu et al., 2018), and to date, no direct evidence for the occurrence of methylotrophic methanogenesis has been documented for lake sediments. Methylotrophic methanogenesis has been shown to be an important pathway mainly in specific marine systems, where methanogens can utilize methylated compounds (e.g., methanol and trimethylamine) as non-competitive substrates for methane production (Xiao et al., 2018; Xu et al., 2021; Zhuang et al., 2018).

The finding that CO<sub>2</sub> reduction pathway dominated methane production throughout the sediment cores at both sites was further supported by the observed apparent fractionation factor  $\alpha_c$  (DS:  $1.071 \pm 0.001$  and PS:  $1.081 \pm 0.001$ ; Fig. 4C, F and Table S1). Rates for CO<sub>2</sub> reduction in Lake Geneva were similar at the two studied sites, but were much higher than those previously reported in other lakes at similar depths (Kuivila et al., 1989). The observed low rates for acetoclastic methanogenesis on the other hand were comparable to those in other lake sediments (Kuivila et al., 1989; Schulz and Conrad, 1996). Methane production via acetate fermentation was traditionally believed to play a more important role than via CO<sub>2</sub> reduction in lake sediments (Whiticar, 1999; Whiticar et al., 1986). However, more recent evidence seems to contradict this paradigm, demonstrating that CO<sub>2</sub> reduction methanogenesis can indeed be a much more significant methane-producing biogeochemical pathway than acetoclastic methanogenesis (Blair et al., 2018; Conrad et al., 2011; Meier et al., 2024). While the dominance of CO<sub>2</sub> reduction methanogenesis in lake sediments has been reported previously, our results reinforce this conclusion with consistent geochemical and isotopic evidence across contrasting sedimentary regimes in Lake Geneva.



At both sites, *Methanoregula* was the most abundant methanogenic genus, particularly in deep sediments where the highest CO<sub>2</sub> reduction rates were observed. This genus, commonly found in freshwater lakes (Bartosiewicz et al., 2024; Berberich et al., 2020; Meier et al., 2024), is known to perform hydrogenotrophic methanogenesis (i.e., CO<sub>2</sub> reduction with hydrogen as the electron donor). *Methanothrix*, the second most abundant methanogen, primarily performs acetoclastic methanogenesis. At PS, *Methanoregula* dominated at all investigated depths, in accordance with high rates of autotrophic methanogenesis. While acetoclastic methanogenesis played only a minor role in total methane production, higher rates were observed for deltaic sediments, with lower apparent fractionation factor. This observation is consistent with higher concentrations of acetate and a higher relative abundance of acetate-consuming *Methanothrix*, suggesting that the pathway of acetoclastic methanogenesis was influenced by both the availability of acetate and the functional methanogenic population. While *Methanothrix* has long been considered to exclusively use acetate as substrate for methanogenesis (Jetten et al., 1992; Smith and Ingram-Smith, 2007), there is now evidence that some species can also perform CO<sub>2</sub> reduction via direct interspecies electron transfer (Rotaru et al., 2014; Zhou et al., 2023).

Although overall methane production rates were similar at both sites, the qPCR data in hand indicated that bulk methane production was not primarily controlled by (i.e., proportional to) the cell abundance of methanogens. Instead, it was likely regulated by other environmental factors, such as limited substrate supply (i.e., H<sub>2</sub> and acetate), stemming from rates of hydrolysis (Kristensen et al., 1995) and/or fermentation rates (Valentine et al., 1994) within the sediments. Since methanogens rely on syntrophic and other heterotrophic bacteria to generate these key substrates, the activity and composition of the broader microbial community may play a significant role in shaping methane production rates (Beulig et al., 2018; Liu and Whitman, 2008). In Lake Geneva sediments, rates of both CO<sub>2</sub> reduction and acetoclastic methanogenesis increased with microbial Shannon diversity. More diverse microbial communities tend to possess more diverse organic matter degradation capacities, resulting in higher production of acetate and H<sub>2</sub>/CO<sub>2</sub>, which in turn promotes overall methane production (Conrad, 2020). In addition, our microbial abundance and diversity data were insufficient to fully characterize the carbon metabolism of microorganisms involved in H<sub>2</sub> and acetate production, which could directly impact CO<sub>2</sub> reduction and acetoclastic methanogenesis and potentially explain the observed methane production

differences. The very low acetate oxidation rates at both sites suggest that differences in methane generation via  $MGR_{DIC}$  versus  $MGR_{Ac}$  may be attributed to the relative availability of methane precursors available (i.e.,  $H_2/CO_2$  versus acetate) (Capone and Kiene, 1988). The acetate concentrations were below 26  $\mu M$  at both sites, but well within the range of what has been measured in profundal sediment of Lake Constance, where acetoclastic methanogenesis was dominant (Schulz and Conrad, 1996). Hence, the consistently low rates of acetoclastic methanogenesis throughout the sediment cores at both sites likely resulted from low turnover rates of acetate during organic matter degradation.

#### **4.3. Effect of organic carbon characteristics on methanogenesis**

Despite the differences in OC sources and quality between the two sites, the overall methane production rates were comparable (Fig. 4B, E and Table S1). However, the sedimentary zones of maximum methane production and the depth-dependent rates of both metabolic modes of methanogenesis varied. This likely reflects differences in OC quality and degradation pathways, which influence the balance between remineralization to  $H_2/CO_2$  versus acetate (Conrad, 2020), resulting in spatial variability in sedimentary methane production.

Potential methane production rates have been shown to correlate positively with the quantity of sediment organic matter (Berberich et al., 2020). However, at both the DS and PS in Lake Geneva, the sediment layers of maximum rates of  $CO_2$  reduction did not coincide with higher TOC contents. Instead, combined rate and isotopic measurements revealed that methanogenesis rates via  $CO_2$  reduction corresponded to less  $^{13}C$ -depleted bulk organic carbon (Fig. 1 and 4). This suggests that the source and microbial decomposition of organic matter, rather than its quantity, primarily influenced the methanogenic activity via the  $CO_2$ -reduction pathway.

Methane production rates in lake sediments can be quite low across various latitudes but can also increase significantly with the addition of fresh organic carbon (Bartosiewicz et al., 2024; Schwarz et al., 2008; West et al., 2012). Indeed, high lipid contents in phytoplankton biomass have been shown to enhance methane production in both engineered systems and lake sediments (West et al., 2015; Zhao et al., 2014). Additionally, existing evidence suggest that terrestrial OC can stimulate methane ebullition in reservoirs (DelSontro et al., 2011; Sobek et al., 2012). It has also been suggested that the availability of easily degradable organic matter controls both

methanogenic pathways and methanogenic archaeal communities (Liu et al., 2017). However, the influence of organic matter source or composition on the relative importance of methane production pathways and their corresponding rates remains poorly constrained and has rarely been explored. At PS, within the zone of high methanogenic activity via CO<sub>2</sub> reduction, TOC became less depleted in <sup>13</sup>C, a trend also observed, though less pronounced, in the deltaic sediments. The δ<sup>13</sup>C shift of TOC within the most active zone at PS likely reflects either the selective loss of isotopically light OM fractions, or changes in organic matter sources, as indicated by depth-related variations in both short- and long-chain fatty acid concentrations.

Contrary to previous studies demonstrating that algal deposition stimulated the activity of acetoclastic methanogens (Schulz and Conrad, 1995; Schwarz et al., 2008), our results revealed higher acetate concentrations in tandem with higher acetoclastic methanogenesis occurring in surface sediments of deltaic site, where high C/N ratios indicated terrestrial inputs. This suggests that allochthonous OC may play a role in acetate production and acetoclastic methanogenesis. However, the apparently much lower overall acetoclastic rates compared CO<sub>2</sub> reduction were likely due to the active acetate consumption via syntrophic oxidation (Conrad et al., 2020). At PS, autochthonous organic matter was the dominant OC source to the sediments, and the CH<sub>4</sub> produced likely resulted from the decomposition of buried algal detritus (Fig. 6). This interpretation is also supported by the 2-fold higher brassicasterol, the 3-fold higher phytol, and 3-4-fold higher long chain fatty acids concentrations (with elevated δ<sup>13</sup>C values) at PS compared to DS. These biomarkers, in combination with lower C/N ratios, are indicative of algal material as the dominant organic contributor to early diagenetic methane production.

While the dominant sedimentary organic matter source (i.e., the partitioning between autochthonous versus allochthonous OM inputs to the sediments) varied between the two studied sites, the similar overall methane production rates imply that methanogenesis occurred ubiquitously in these lacustrine sediments, independent of the OC sources, their apparent susceptibility to organic matter degradation, and/or their overall diagenetic state. This finding aligns with a recent study across the river/deltaic-pelagic continuum in a reservoir system in southwest Ohio (Berberich et al., 2020), and holds important implications for understanding the lacustrine methane cycle. On the one hand, eutrophication in lakes and other aquatic systems often increases the supply of autochthonous organic carbon, thereby enhancing methanogenesis and leading to

increased methane emissions (Davidson et al., 2018). On the other hand, the potential of terrestrial organic matter to contribute to lacustrine methane production can be significantly impacted by anthropogenic activities, such as dam construction (Li et al., 2023), or as a result of deforestation and soil erosion, which alter sediment inputs into the lake (Bélanger et al., 2017). Our study demonstrates that diverse OC sources and varying diagenetic states in both profundal and deltaic sediments support substantial rates of methane formation through CO<sub>2</sub> reduction. However, identifying the exact fractions of organic matter that were degraded and fueled methane production remains challenging. While acetoclastic methanogenesis appears to be relevant to the breakdown and decomposition of terrestrial organic matter that favors acetate production and accumulation in deltaic sediments, the sources of organic carbon driving the more dominant CO<sub>2</sub>-reducing methanogenesis in the studied sediments remains unclear. The key environmental factors controlling the organic matter degradation in methanogenic sediments remain unresolved and require further investigation. Understanding these mechanisms is essential for predicting how changes in organic carbon inputs and sediment dynamics may influence methane production and emissions from lacustrine environments.

## 5. Conclusions

Our study demonstrates that both profundal and deltaic sediments of Lake Geneva are significant sources of methane, despite clear differences in origins and compositions of organic matter. The profundal site is dominated by aquatic OM, while the deltaic site features a more variable mix of OM sources, including substantial terrestrial contributions at certain depths. Methane production at both sites is driven by CO<sub>2</sub> reduction, which accounted for over 95% of total methane production and was most probably mediated by *Methanoregula*. While phylogenetic data suggest a link between methanogen communities and methanogenetic pathways, the broader microbial community dynamics, particularly those involved in H<sub>2</sub> and acetate production, remain insufficiently understood.

At the profundal site, methane production is mainly associated with the decomposition of aquatic organic matter, as terrestrial OC is less abundant. At the deltaic site, acetoclastic methanogenesis appears linked to the higher terrestrial organic matter inputs. Nevertheless, the overall dominance of methanogenesis via CO<sub>2</sub>

808 reduction at both sites suggests that depositional regime, as well as OM source and  
809 composition are not the primary determinants of the prevailing methane producing  
810 pathway. Instead, other environmental factors such as substrate availability or  
811 microbial community dynamics may influence methane production, although the  
812 specific mechanisms remain uncertain. For example, the sample-specific molecular  
813 composition of sedimentary organic matter could be important in determining which  
814 substrate, H<sub>2</sub> and acetate, is the main substrates for methanogenesis. Future research  
815 should focus on unraveling these interactions to better predict if, and how, changes in  
816 OM inputs and sediment dynamics may impact methane emissions from lacustrine  
817 environments.

## **Data availability statement**

Raw reads of the 16S rRNA sequencing data are available on NCBI GenBank with BioProject ID PRJNA736863, under accession number SRR14794332- SRR14794339.

## **Author contributions**

CJS, GS and MAL conceived the research. CJS acquired funding for this study. GS performed field work, lab experiments and data analyses. JT assisted with Pyrolysis-GC data analysis. CG and MAL measured porewater volatile fatty acids and analyzed the data. JZ and MFL supported rate measurements and molecular analyses. GS wrote the original draft of the manuscript. All authors helped to revise and approved the submitted version.

## **Acknowledgements**

This research was supported by Eawag internal funds. We thank Alois Zwyssig, Sandra Schmid and Cameron Callbeck for assistance with field sample collection. We also thank Serge Robert for laboratory assistance including lipid sample preparation and laboratory analyses and for his help in elemental analysis of samples. Patrick Kathriner is acknowledged for laboratory support. We are also grateful to Thomas Kuhn at the University of Basel for laboratory support with the radioisotope measurements.

## **Competing interests**

At least one of the (co-)authors is a member of the editorial board of Biogeosciences.

## 844    **References**

- 845    Bartosiewicz, M., Przytulska, A., Birkholz, A., Zopfi, J., and Lehmann, M. F.:  
846    Controls and significance of priming effects in lake sediments, *Glob Chang Biol*,  
847    30, 1–13, <https://doi.org/10.1111/gcb.17076>, 2024.
- 848    Bastviken, D., Tranvik, L. J., Downing, J. A., Crill, P. M., and Enrich-Prast, A.:  
849    Freshwater methane emissions offset the continental carbon sink, *Science*  
850    (1979), 331, 50–50, <https://doi.org/10.1126/science.1196808>, 2011.
- 851    Bechtel, A. and Schubert, C. J.: A biogeochemical study of sediments from the  
852    eutrophic Lake Lugano and the oligotrophic Lake Brienz, Switzerland, *Org*  
853    *Geochem*, 40, 1100–1114, <https://doi.org/10.1016/j.orggeochem.2009.06.009>,  
854    2009.
- 855    Bélanger, É., Lucotte, M., Moingt, M., Paquet, S., Oestreicher, J., and Rozon, C.:  
856    Altered nature of terrestrial organic matter transferred to aquatic systems  
857    following deforestation in the Amazon, *Applied Geochemistry*, 87, 136–145,  
858    <https://doi.org/10.1016/j.apgeochem.2017.10.016>, 2017.
- 859    Berberich, M. E., Beaulieu, J. J., Hamilton, T. L., Waldo, S., and Buffam, I.: Spatial  
860    variability of sediment methane production and methanogen communities  
861    within a eutrophic reservoir: Importance of organic matter source and quantity,  
862    *Limnol Oceanogr*, 65, 1336–1358, <https://doi.org/10.1002/lno.11392>, 2020.
- 863    Beulig, F., Røy, H., Glombitza, C., and Jørgensen, B. B.: Control on rate and  
864    pathway of anaerobic organic carbon degradation in the seabed, *Proc Natl Acad*  
865    *Sci USA*, 115, 367–372, <https://doi.org/10.1073/pnas.1715789115>, 2018.
- 866    Blair, N. E., Leithold, E. L., Thanos Papanicolaou, A. N., Wilson, C. G., Keefer, L.,  
867    Kirton, E., Vinson, D., Schnoebelen, D., Rhoads, B., Yu, M., and Lewis, Q.: The C-  
868    biogeochemistry of a Midwestern USA agricultural impoundment in context:  
869    Lake Decatur in the intensively managed landscape critical zone observatory,  
870    *Biogeochemistry*, 138, 171–195, <https://doi.org/10.1007/s10533-018-0439-9>,  
871    2018.
- 872    Burrus, D., Thomas, R. L., Dominik, J., and Vernet, J.-P.: Recovery and  
873    concentration of suspended solids in the upper Rhone River by continuous flow  
874    centrifugation, *Hydrol Process*, 3, 65–74,  
875    <https://doi.org/10.1002/hyp.3360030107>, 1989.
- 876    Capone, D. G. and Kiene, R. P.: Comparison of microbial dynamics in marine and  
877    freshwater sediments: Contrasts in anaerobic carbon catabolism, *Limnol*  
878    *Oceanogr*, 33, 725–749, <https://doi.org/10.4319/lo.1988.33.4part2.0725>, 1988.
- 879    Chikaraishi, Y., Naraoka, H., and Poulson, S. R.: Hydrogen and carbon isotopic  
880    fractionations of lipid biosynthesis among terrestrial (C3, C4 and CAM) and  
881    aquatic plants, *Phytochemistry*, 65, 1369–1381,  
882    <https://doi.org/10.1016/j.phytochem.2004.03.036>, 2004.
- 883    Cloern, J. E., Canuel, E. A., and Harris, D.: Stable carbon and nitrogen isotope  
884    composition of aquatic and terrestrial plants of the San Francisco Bay estuarine  
885    system, *Limnol Oceanogr*, 47, 713–729,  
886    <https://doi.org/10.4319/lo.2002.47.3.0713>, 2002.
- 887    Conrad, R.: Quantification of methanogenic pathways using stable carbon  
888    isotopic signatures: a review and a proposal, *Org Geochem*, 36, 739–752,  
889    <https://doi.org/10.1016/j.orggeochem.2004.09.006>, 2005.
- 890    Conrad, R.: Importance of hydrogenotrophic, acetoclastic and methylotrophic  
891    methanogenesis for methane production in terrestrial, aquatic and other anoxic

892 environments: A mini review, *Pedosphere*, 30, 25–39,  
 893 [https://doi.org/10.1016/S1002-0160\(18\)60052-9](https://doi.org/10.1016/S1002-0160(18)60052-9), 2020.  
 894 Conrad, R., Noll, M., Claus, P., Klose, M., Bastos, W. R., and Enrich-Prast, A.: Stable  
 895 carbon isotope discrimination and microbiology of methane formation in  
 896 tropical anoxic lake sediments, *Biogeosciences*, 8, 795–814,  
 897 <https://doi.org/10.5194/bg-8-795-2011>, 2011.  
 898 Conrad, R., Klose, M., and Enrich-Prast, A.: Acetate turnover and methanogenic  
 899 pathways in Amazonian lake sediments, *Biogeosciences*, 17, 1063–1069,  
 900 <https://doi.org/10.5194/bg-17-1063-2020>, 2020.  
 901 Cranwell, P. A.: Monocarboxylic acids in lake sediments: Indicators, derived from  
 902 terrestrial and aquatic biota, of paleoenvironmental trophic levels, *Chem Geol*,  
 903 14, 1–14, [https://doi.org/10.1016/0009-2541\(74\)90092-8](https://doi.org/10.1016/0009-2541(74)90092-8), 1974.  
 904 Cranwell, P. A.: Decomposition of aquatic biota and sediment formation: organic  
 905 compounds in detritus resulting from microbial attack on the alga *Ceratium*  
 906 *hirundinella*, *Freshw Biol*, 6, 41–48, [https://doi.org/10.1111/j.1365-](https://doi.org/10.1111/j.1365-2427.1976.tb01589.x)  
 907 [2427.1976.tb01589.x](https://doi.org/10.1111/j.1365-2427.1976.tb01589.x), 1976.  
 908 Dai, J., Sun, M.-Y., Culp, R. A., and Noakes, J. E.: Changes in chemical and isotopic  
 909 signatures of plant materials during degradation: Implication for assessing  
 910 various organic inputs in estuarine systems, *Geophys Res Lett*, 32, L13608,  
 911 <https://doi.org/10.1029/2005GL023133>, 2005.  
 912 Davidson, T. A., Audet, J., Jeppesen, E., Landkildehus, F., Lauridsen, T. L.,  
 913 Søndergaard, M., and Syväranta, J.: Synergy between nutrients and warming  
 914 enhances methane ebullition from experimental lakes, *Nat Clim Chang*, 8, 156–  
 915 160, <https://doi.org/10.1038/s41558-017-0063-z>, 2018.  
 916 Dean, W. E. and Gorham, E.: Magnitude and significance of carbon burial in lakes,  
 917 reservoirs, and peatlands, *Geology*, 26, 535, <https://doi.org/10.3133/fs05899>,  
 918 1998.  
 919 DelSontro, T., Kunz, M. J., Kempter, T., Wüest, A., Wehrli, B., and Senn, D. B.:  
 920 Spatial heterogeneity of methane ebullition in a large tropical reservoir, *Environ*  
 921 *Sci Technol*, 45, 9866–9873, <https://doi.org/10.1021/es2005545>, 2011.  
 922 Demirel, B. and Scherer, P.: The roles of acetotrophic and hydrogenotrophic  
 923 methanogens during anaerobic conversion of biomass to methane: a review, *Rev*  
 924 *Environ Sci Biotechnol*, 7, 173–190, [https://doi.org/10.1007/s11157-008-9131-](https://doi.org/10.1007/s11157-008-9131-1)  
 925 [1](https://doi.org/10.1007/s11157-008-9131-1), 2008.  
 926 Downing, J. A., Prairie, Y. T., Cole, J. J., Duarte, C. M., Tranvik, L. J., Striegl, R. G.,  
 927 McDowell, W. H., Kortelainen, P., Caraco, N. F., Melack, J. M., and Middelburg, J. J.:  
 928 The global abundance and size distribution of lakes, ponds, and impoundments,  
 929 *Limnol Oceanogr*, 51, 2388–2397, <https://doi.org/10.4319/lo.2006.51.5.2388>,  
 930 2006.  
 931 Eglinton, G. and Hamilton, R. J.: Leaf epicuticular waxes, *Science* (1979), 156,  
 932 1322–1335, <https://doi.org/10.1126/science.156.3780.1322>, 1967.  
 933 Ernst, L., Steinfeld, B., Barayeu, U., Klintzsch, T., Kurth, M., Grimm, D., Dick, T. P.,  
 934 Rebele, J. G., Bischofs, I. B., and Keppler, F.: Methane formation driven by  
 935 reactive oxygen species across all living organisms, *Nature*, 603, 482–487,  
 936 <https://doi.org/10.1038/s41586-022-04511-9>, 2022.  
 937 Ficken, K. J., Li, B., Swain, D. L., and Eglinton, G.: An n-alkane proxy for the  
 938 sedimentary input of submerged/floating freshwater aquatic macrophytes, *Org*  
 939 *Geochem*, 31, 745–749, [https://doi.org/10.1016/S0146-6380\(00\)00081-4](https://doi.org/10.1016/S0146-6380(00)00081-4),  
 940 2000.



941 Gallina, N., Beniston, M., and Jacquet, S.: Estimating future cyanobacterial  
 942 occurrence and importance in lakes: a case study with *Planktothrix rubescens* in  
 943 Lake Geneva, Aquat Sci, 79, 249–263, [https://doi.org/10.1007/s00027-016-](https://doi.org/10.1007/s00027-016-0494-z)  
 944 0494-z, 2017.  
 945 Glombitza, C., Pedersen, J., Røy, H., and Jørgensen, B. B.: Direct analysis of volatile  
 946 fatty acids in marine sediment porewater by two-dimensional ion  
 947 chromatography-mass spectrometry, Limnol Oceanogr Methods, 12, 455–468,  
 948 <https://doi.org/10.4319/lom.2014.12.455>, 2014.  
 949 Grasset, C., Mendonça, R., Villamor Saucedo, G., Bastviken, D., Roland, F., and  
 950 Sobek, S.: Large but variable methane production in anoxic freshwater sediment  
 951 upon addition of allochthonous and autochthonous organic matter, Limnol  
 952 Oceanogr, 63, 1488–1501, <https://doi.org/10.1002/lno.10786>, 2018.  
 953 Han, X., Schubert, C. J., Fiskal, A., Dubois, N., and Lever, M. A.: Eutrophication as a  
 954 driver of microbial community structure in lake sediments, Environ Microbiol,  
 955 22, 3446–3462, <https://doi.org/10.1111/1462-2920.15115>, 2020.  
 956 Han, X., Tolu, J., Deng, L., Fiskal, A., Schubert, C. J., Winkel, L. H. E., and Lever, M.  
 957 A.: Long-term preservation of biomolecules in lake sediments: potential  
 958 importance of physical shielding by recalcitrant cell walls, PNAS Nexus, 1,  
 959 <https://doi.org/10.1093/pnasnexus/pgac076>, 2022.  
 960 Hansen, L. K., Jakobsen, R., and Postma, D.: Methanogenesis in a shallow sandy  
 961 aquifer, Rømø, Denmark, Geochim Cosmochim Acta, 65, 2925–2935,  
 962 [https://doi.org/10.1016/S0016-7037\(01\)00653-6](https://doi.org/10.1016/S0016-7037(01)00653-6), 2001.  
 963 Hedges, J. I., Clark, W. A., Quay, P. D., Richey, J. E., Devol, A. H., and Santos, M.:  
 964 Compositions and fluxes of particulate organic material in the Amazon River,  
 965 Limnol Oceanogr, 31, 717–738, <https://doi.org/10.4319/lo.1986.31.4.0717>,  
 966 1986.  
 967 Jetten, M. S. M., Stams, A. J. M., and Zehnder, A. J. B.: Methanogenesis from acetate:  
 968 a comparison of the acetate metabolism in *Methanothrix soehngenii* and  
 969 *Methanosarcina* spp., FEMS Microbiol Lett, 88, 181–198,  
 970 <https://doi.org/10.1111/j.1574-6968.1992.tb04987.x>, 1992.  
 971 Kawamura, K., Ishiwatari, R., and Ogura, K.: Early diagenesis of organic matter in  
 972 the water column and sediments: Microbial degradation and resynthesis of lipids  
 973 in Lake Haruna, Org Geochem, 11, 251–264, [https://doi.org/10.1016/0146-](https://doi.org/10.1016/0146-6380(87)90036-2)  
 974 6380(87)90036-2, 1987.  
 975 Kristensen, E., Ahmed, S. I., and Devol, A. H.: Aerobic and anaerobic  
 976 decomposition of organic matter in marine sediment: Which is fastest?, Limnol  
 977 Oceanogr, 40, 1430–1437, <https://doi.org/10.4319/lo.1995.40.8.1430>, 1995.  
 978 Kuivila, K. M., Murray, J. W., Devol, A. H., and Novelli, P. C.: Methane production,  
 979 sulfate reduction and competition for substrates in the sediments of Lake  
 980 Washington, Geochim Cosmochim Acta, 53, 409–416,  
 981 [https://doi.org/10.1016/0016-7037\(89\)90392-X](https://doi.org/10.1016/0016-7037(89)90392-X), 1989.  
 982 Ladd, S. N., Nelson, D. B., Schubert, C. J., and Dubois, N.: Lipid compound classes  
 983 display diverging hydrogen isotope responses in lakes along a nutrient gradient,  
 984 Geochim Cosmochim Acta, 237, 103–119,  
 985 <https://doi.org/10.1016/j.gca.2018.06.005>, 2018.  
 986 Lamb, A. L., Wilson, G. P., and Leng, M. J.: A review of coastal palaeoclimate and  
 987 relative sea-level reconstructions using  $\delta^{13}\text{C}$  and C/N ratios in organic material,  
 988 Earth Sci Rev, 75, 29–57, <https://doi.org/10.1016/j.earscirev.2005.10.003>, 2006.

989 Larsen, S., Andersen, T., and Hessen, D. O.: Climate change predicted to cause  
 990 severe increase of organic carbon in lakes, *Glob Chang Biol*, 17, 1186–1192,  
 991 <https://doi.org/10.1111/j.1365-2486.2010.02257.x>, 2011.  
 992 Lehmann, M. F., Bernasconi, S. M., Barbieri, A., and McKenzie, J. A.: Preservation  
 993 of organic matter and alteration of its carbon and nitrogen isotope composition  
 994 during simulated and in situ early sedimentary diagenesis, *Geochim Cosmochim*  
 995 *Acta*, 66, 3573–3584, [https://doi.org/10.1016/S0016-7037\(02\)00968-7](https://doi.org/10.1016/S0016-7037(02)00968-7), 2002.  
 996 Lehmann, M. F., Carstens, D., Deek, A., McCarthy, M., Schubert, C. J., and Zopfi, J.:  
 997 Amino acid and amino sugar compositional changes during in vitro degradation  
 998 of algal organic matter indicate rapid bacterial re-synthesis, *Geochim Cosmochim*  
 999 *Acta*, 283, 67–84, <https://doi.org/10.1016/j.gca.2020.05.025>, 2020.  
 1000 Lever, M. A. and Teske, A. P.: Diversity of methane-cycling archaea in  
 1001 hydrothermal sediment investigated by general and group-specific PCR primers,  
 1002 *Appl Environ Microbiol*, 81, 1426–1441, [https://doi.org/10.1128/AEM.03588-](https://doi.org/10.1128/AEM.03588-14)  
 1003 14, 2015.  
 1004 Li, B., Wang, H., Lai, A., Xue, J., Wu, Q., Yu, C., Xie, K., Mao, Z., Li, H., Xing, P., and  
 1005 Wu, Q. L.: Hydrogenotrophic pathway dominates methanogenesis along the  
 1006 river-estuary continuum of the Yangtze River, *Water Res*, 240, 120096,  
 1007 <https://doi.org/10.1016/j.watres.2023.120096>, 2023.  
 1008 Liu, Y. and Whitman, W. B.: Metabolic, Phylogenetic, and Ecological Diversity of  
 1009 the Methanogenic Archaea, *Ann N Y Acad Sci*, 1125, 171–189,  
 1010 <https://doi.org/10.1196/annals.1419.019>, 2008.  
 1011 Liu, Y., Conrad, R., Yao, T., Gleixner, G., and Claus, P.: Change of methane  
 1012 production pathway with sediment depth in a lake on the Tibetan plateau,  
 1013 *Palaeogeogr Palaeoclimatol Palaeoecol*, 474, 279–286,  
 1014 <https://doi.org/10.1016/j.palaeo.2016.06.021>, 2017.  
 1015 Lyu, Z., Shao, N., Akinyemi, T., and Whitman, W. B.: Methanogenesis, *Current*  
 1016 *Biology*, 28, R727–R732, <https://doi.org/10.1016/j.cub.2018.05.021>, 2018.  
 1017 Masson-Delmotte, V., Zhai, P., Pirani, A., Connors, S. L., Péan, C., Berger, S., Caud,  
 1018 N., Chen, Y., Goldfarb, L., and Gomis, M. I.: Climate change 2021: the physical  
 1019 science basis, Contribution of working group I to the sixth assessment report of  
 1020 the intergovernmental panel on climate change, 2, 2391, 2021.  
 1021 McMurdie, P. J. and Holmes, S.: Phyloseq: an R package for reproducible  
 1022 interactive analysis and graphics of microbiome census data, *PLoS One*, 8, 1–11,  
 1023 <https://doi.org/10.1371/journal.pone.0061217>, 2013.  
 1024 Meier, D., van Grinsven, S., Michel, A., Eickenbusch, P., Glombitza, C., Han, X.,  
 1025 Fiskal, A., Bernasconi, S., Schubert, C. J., and Lever, M. A.: Hydrogen-independent  
 1026 CO<sub>2</sub> reduction dominates methanogenesis in five temperate lakes that differ in  
 1027 trophic states, *ISME Communications*, 4,  
 1028 <https://doi.org/10.1093/ismeco/ycae089>, 2024.  
 1029 Mendonça, R., Müller, R. A., Clow, D., Verpoorter, C., Raymond, P., Tranvik, L. J.,  
 1030 and Sobek, S.: Organic carbon burial in global lakes and reservoirs, *Nat Commun*,  
 1031 8, 1–6, <https://doi.org/10.1038/s41467-017-01789-6>, 2017.  
 1032 Meyers, P. A.: Preservation of elemental and isotopic source identification of  
 1033 sedimentary organic matter, *Chem Geol*, 114, 289–302,  
 1034 [https://doi.org/10.1016/0009-2541\(94\)90059-0](https://doi.org/10.1016/0009-2541(94)90059-0), 1994.  
 1035 Meyers, P. A. and Ishiwatari, R.: Lacustrine organic geochemistry-an overview of  
 1036 indicators of organic matter sources and diagenesis in lake sediments, *Org*  
 1037 *Geochem*, 20, 867–900, [https://doi.org/10.1016/0146-6380\(93\)90100-P](https://doi.org/10.1016/0146-6380(93)90100-P), 1993.

1038 Meyers, P. A. and Takeuchi, N.: Environmental changes in Saginaw Bay, Lake  
1039 Huron recorded by geolipid contents of sediments deposited since 1800,  
1040 Environmental Geology, 3, 257–266, <https://doi.org/10.1007/BF02473517>,  
1041 1981.

1042 O’Leary, M. H.: Carbon isotope fractionation in plants, Phytochemistry, 20, 553–  
1043 567, [https://doi.org/10.1016/0031-9422\(81\)85134-5](https://doi.org/10.1016/0031-9422(81)85134-5), 1981.

1044 Opsahl, S. and Benner, R.: Early diagenesis of vascular plant tissues: Lignin and  
1045 cutin decomposition and biogeochemical implications, Geochim Cosmochim  
1046 Acta, 59, 4889–4904, [https://doi.org/10.1016/0016-7037\(95\)00348-7](https://doi.org/10.1016/0016-7037(95)00348-7), 1995.

1047 Parsons, T. R., Stephens, K., and Strickland, J. D. H.: On the Chemical Composition  
1048 of Eleven Species of Marine Phytoplankters, Journal of the Fisheries Research  
1049 Board of Canada, 18, 1001–1016, <https://doi.org/10.1139/f61-063>, 1961.

1050 R Core Team: A Language and Environment for Statistical Computing. (R  
1051 Foundation for Statistical Computing) [online], [www.r-project.org/](http://www.r-project.org/), 2024.

1052 Randlett, M.-E., Sollberger, S., Del Sontro, T., Müller, B., Corella, J. P., Wehrli, B.,  
1053 and Schubert, C. J.: Mineralization pathways of organic matter deposited in a  
1054 river–lake transition of the Rhone River Delta, Lake Geneva, Environ Sci Process  
1055 Impacts, 17, 370–380, <https://doi.org/10.1039/C4EM00470A>, 2015.

1056 Raymond, P. A. and Bauer, J. E.: Riverine export of aged terrestrial organic matter  
1057 to the North Atlantic Ocean, Nature, 409, 497–500,  
1058 <https://doi.org/10.1038/35054034>, 2001.

1059 Ritalahti, K. M., Amos, B. K., Sung, Y., Wu, Q., Koenigsberg, S. S., and Löffler, F. E.:  
1060 Quantitative PCR targeting 16S rRNA and reductive dehalogenase genes  
1061 simultaneously monitors multiple *Dehalococcoides* strains, Appl Environ  
1062 Microbiol, 72, 2765–2774, <https://doi.org/10.1128/AEM.72.4.2765-2774.2006>,  
1063 2006.

1064 Rotaru, A.-E., Shrestha, P. M., Liu, F., Shrestha, M., Shrestha, D., Embree, M.,  
1065 Zengler, K., Wardman, C., Nevin, K. P., and Lovley, D. R.: A new model for electron  
1066 flow during anaerobic digestion: direct interspecies electron transfer to  
1067 Methanosaeta for the reduction of carbon dioxide to methane, Energy Environ.  
1068 Sci., 7, 408–415, <https://doi.org/10.1039/C3EE42189A>, 2014.

1069 Schaedler, F., Lockwood, C., Lueder, U., Glombitza, C., Kappler, A., and Schmidt, C.:  
1070 Microbially mediated coupling of Fe and N cycles by nitrate-reducing Fe (II)-  
1071 oxidizing bacteria in littoral freshwater sediments, Appl Environ Microbiol, 84,  
1072 1–14, <https://doi.org/10.1128/AEM.02013-17>, 2018.

1073 Schellekens, J., Buurman, P., and Pontevedra-Pombal, X.: Selecting parameters for  
1074 the environmental interpretation of peat molecular chemistry – A pyrolysis-  
1075 GC/MS study, Org Geochem, 40, 678–691,  
1076 <https://doi.org/10.1016/j.orggeochem.2009.03.006>, 2009.

1077 Schubert, C. J. and Nielsen, B.: Effects of decarbonation treatments on  $\delta^{13}\text{C}$  values  
1078 in marine sediments, Mar Chem, 72, 55–59, [https://doi.org/10.1016/S0304-4203\(00\)00066-9](https://doi.org/10.1016/S0304-4203(00)00066-9), 2000.

1080 Schulz, S. and Conrad, R.: Effect of algal deposition on acetate and methane  
1081 concentrations in the profundal sediment of a deep lake (Lake Constance), FEMS  
1082 Microbiol Ecol, 16, 251–259, [https://doi.org/10.1016/0168-6496\(94\)00088-E](https://doi.org/10.1016/0168-6496(94)00088-E),  
1083 1995.

1084 Schulz, S. and Conrad, R.: Influence of temperature on pathways to methane  
1085 production in the permanently cold profundal sediment of Lake Constance, FEMS

1086 Microbiol Ecol, 20, 1–14, [https://doi.org/10.1016/0168-6496\(96\)00009-8](https://doi.org/10.1016/0168-6496(96)00009-8),  
1087 1996.

1088 Schwarz, J. I. K. K., Eckert, W., and Conrad, R.: Response of the methanogenic  
1089 microbial community of a profundal lake sediment (Lake Kinneret, Israel) to  
1090 algal deposition, Limnol Oceanogr, 53, 113–121,  
1091 <https://doi.org/10.4319/lo.2008.53.1.0113>, 2008.

1092 Shi, W., Sun, M. Y., Molina, M., and Hodson, R. E.: Variability in the distribution of  
1093 lipid biomarkers and their molecular isotopic composition in Altamaha estuarine  
1094 sediments: Implications for the relative contribution of organic matter from  
1095 various sources, Org Geochem, 32, 453–467, [https://doi.org/10.1016/S0146-](https://doi.org/10.1016/S0146-6380(00)00189-3)  
1096 6380(00)00189-3, 2001.

1097 Smith, K. S. and Ingram-Smith, C.: Methanosaeta, the forgotten methanogen?,  
1098 Trends Microbiol, 15, 150–155, <https://doi.org/10.1016/j.tim.2007.02.002>,  
1099 2007.

1100 Sobek, S., Durisch-Kaiser, E., Zurbrugg, R., Wongfun, N., Wessels, M., Pasche, N.,  
1101 and Wehrli, B.: Organic carbon burial efficiency in lake sediments controlled by  
1102 oxygen exposure time and sediment source, Limnol Oceanogr, 54, 2243–2254,  
1103 <https://doi.org/10.4319/lo.2009.54.6.2243>, 2009.

1104 Sobek, S., DelSontro, T., Wongfun, N., and Wehrli, B.: Extreme organic carbon  
1105 burial fuels intense methane bubbling in a temperate reservoir, Geophys Res  
1106 Lett, 39, 2–5, <https://doi.org/10.1029/2011GL050144>, 2012.

1107 Sollberger, S., Corella, J. P., Girardclos, S., Randlett, M. E., Schubert, C. J., Senn, D.  
1108 B., Wehrli, B., and DelSontro, T.: Spatial heterogeneity of benthic methane  
1109 dynamics in the subaquatic canyons of the Rhone River Delta (Lake Geneva),  
1110 Aquat Sci, 76, 89–101, <https://doi.org/10.1007/s00027-013-0319-2>, 2014.

1111 Su, G., Niemann, H., Steinle, L., Zopfi, J., and Lehmann, M. F.: Evaluating  
1112 radioisotope-based approaches to measure anaerobic methane oxidation rates in  
1113 lacustrine sediments, Limnol Oceanogr Methods, 17, 429–438,  
1114 <https://doi.org/10.1002/lom3.10323>, 2019.

1115 Su, G., Zopfi, J., Yao, H., Steinle, L., Niemann, H., and Lehmann, M. F.:  
1116 Manganese/iron-supported sulfate-dependent anaerobic oxidation of methane  
1117 by archaea in lake sediments, Limnol Oceanogr, 65, 863–875,  
1118 <https://doi.org/10.1002/lno.11354>, 2020.

1119 Su, G., Lehmann, M. F., Tischer, J., Weber, Y., Lepori, F., Walser, J.-C., Niemann, H.,  
1120 and Zopfi, J.: Water column dynamics control nitrite-dependent anaerobic  
1121 methane oxidation by *Candidatus* “Methyloirabilis” in stratified lake basins,  
1122 ISME J, 17, 693–702, <https://doi.org/10.1038/s41396-023-01382-4>, 2023.

1123 Tolu, J., Gerber, L., Boily, J.-F., and Bindler, R.: High-throughput characterization  
1124 of sediment organic matter by pyrolysis–gas chromatography/mass  
1125 spectrometry and multivariate curve resolution: A promising analytical tool in  
1126 (paleo)limnology, Anal Chim Acta, 880, 93–102,  
1127 <https://doi.org/10.1016/j.aca.2015.03.043>, 2015.

1128 Tolu, J., Rydberg, J., Meyer-Jacob, C., Gerber, L., and Bindler, R.: Spatial variability  
1129 of organic matter molecular composition and elemental geochemistry in surface  
1130 sediments of a small boreal Swedish lake, Biogeosciences, 14, 1773–1792,  
1131 <https://doi.org/10.5194/bg-14-1773-2017>, 2017.

1132 Valentine, D. W., Holland, E. A., and Schimel, D. S.: Ecosystem and physiological  
1133 controls over methane production in northern wetlands, J Geophys Res, 99,  
1134 1563, <https://doi.org/10.1029/93JD00391>, 1994.

1135 Volkman, J. K.: A review of sterol markers for marine and terrigenous organic  
 1136 matter, *Org Geochem*, 9, 83–99, [https://doi.org/10.1016/0146-6380\(86\)90089-](https://doi.org/10.1016/0146-6380(86)90089-6)  
 1137 6, 1986.

1138 Volkman, J. K., Johns, R. B., Gillan, F. T., Perry, G. J., and Bavor, H. J.: Microbial  
 1139 lipids of an intertidal sediment—I. Fatty acids and hydrocarbons, *Geochim*  
 1140 *Cosmochim Acta*, 44, 1133–1143, [https://doi.org/10.1016/0016-](https://doi.org/10.1016/0016-7037(80)90067-8)  
 1141 7037(80)90067-8, 1980.

1142 Volkman, J. K., Barrett, S. M., Blackburn, S. I., Mansour, M. P., Sikes, E. L., and Gelin,  
 1143 F.: Microalgal biomarkers: A review of recent research developments, *Org*  
 1144 *Geochem*, 29, 1163–1179, [https://doi.org/10.1016/S0146-6380\(98\)00062-X](https://doi.org/10.1016/S0146-6380(98)00062-X),  
 1145 1998.

1146 West, W. E., Coloso, J. J., and Jones, S. E.: Effects of algal and terrestrial carbon on  
 1147 methane production rates and methanogen community structure in a temperate  
 1148 lake sediment, *Freshw Biol*, 57, 949–955, [https://doi.org/10.1111/j.1365-](https://doi.org/10.1111/j.1365-2427.2012.02755.x)  
 1149 2427.2012.02755.x, 2012.

1150 West, W. E., McCarthy, S. M., and Jones, S. E.: Phytoplankton lipid content  
 1151 influences freshwater lake methanogenesis, *Freshw Biol*, 2261–2269,  
 1152 <https://doi.org/10.1111/fwb.12652>, 2015.

1153 Whiticar, M. J.: Carbon and hydrogen isotope systematics of bacterial formation  
 1154 and oxidation of methane, *Chem Geol*, 161, 291–314,  
 1155 [https://doi.org/10.1016/S0009-2541\(99\)00092-3](https://doi.org/10.1016/S0009-2541(99)00092-3), 1999.

1156 Whiticar, M. J. J., Faber, E., and Schoell, M.: Biogenic methane formation in marine  
 1157 and freshwater environments: CO<sub>2</sub> reduction vs. acetate fermentation—Isotope  
 1158 evidence, *Geochim Cosmochim Acta*, 50, 693–709,  
 1159 [https://doi.org/10.1016/0016-7037\(86\)90346-7](https://doi.org/10.1016/0016-7037(86)90346-7), 1986.

1160 Xiao, K.-Q., Beulig, F., Røy, H., Jørgensen, B. B., and Risgaard-Petersen, N.:  
 1161 Methylothetic methanogenesis fuels cryptic methane cycling in marine surface  
 1162 sediment, *Limnol Oceanogr*, 63, 1519–1527, <https://doi.org/10.1002/lno.10788>,  
 1163 2018.

1164 Xu, L., Zhuang, G. C., Montgomery, A., Liang, Q., Joye, S. B., and Wang, F.: Methyl-  
 1165 compounds driven benthic carbon cycling in the sulfate-reducing sediments of  
 1166 South China Sea, *Environ Microbiol*, 23, 641–651,  
 1167 <https://doi.org/10.1111/1462-2920.15110>, 2021.

1168 Zhao, B., Ma, J., Zhao, Q., Laurens, L., Jarvis, E., Chen, S., and Frear, C.: Efficient  
 1169 anaerobic digestion of whole microalgae and lipid-extracted microalgae residues  
 1170 for methane energy production, *Bioresour Technol*, 161, 423–430,  
 1171 <https://doi.org/10.1016/j.biortech.2014.03.079>, 2014.

1172 Zhou, J., Smith, J. A., Li, M., and Holmes, D. E.: Methane production by  
 1173 *Methanothrix thermoacetophila* via direct interspecies electron transfer with  
 1174 *Geobacter metallireducens*, *mBio*, 2–3, <https://doi.org/10.1128/mbio.00360-23>,  
 1175 2023.

1176 Zhuang, G.-C., Heuer, V. B., Lazar, C. S., Goldhammer, T., Wendt, J., Samarkin, V. A.,  
 1177 Elvert, M., Teske, A. P., Joye, S. B., and Hinrichs, K.-U.: Relative importance of  
 1178 methylothetic methanogenesis in sediments of the Western Mediterranean Sea,  
 1179 *Geochim Cosmochim Acta*, 224, 171–186,  
 1180 <https://doi.org/10.1016/j.gca.2017.12.024>, 2018.